COLLEGE OF EPS

Low Temperature Plasma Surface Modification of Stainless Steels for Ice Sliding Applications

Andrew du Plessis

Supervisor: Professor H. Dong

Co-Supervisor: Dr J. Chen

WORD COUNT; 14,707

Contents

1 Introduction

The aim of this research project is to investigate the effect of plasma surface modification on the stainless steels currently used in the blades of ice skates, and those which may prove an attractive alternative in the future. Currently blades are subjected to an in service environment which exposes them to severe wear situations, during ice sliding. This can present itself as an issue for several reasons, wear on the blades results in a loss of edge sharpness and an increase in friction with an associated loss in glide performance. The aforementioned are important for both the recreational skater and for high level athletes, who demand the very best in performance from their equipment[1, 2].

Damage to the blade can occur as a result of common wear mechanisms experienced during sliding, such as adhesive and abrasive wear. This may occur during the sliding itself or as a result of repeated impact with the ice during touch-down of the skate during the natural cycle. Issues related to damage brought about through damage to the wear and hardness properties of a material, are termed tribological issues. Recently much work has been put into developing methods of reducing the impact of this through the application of technologies such as surface engineering, either in the form of surface coating treatments or surface modification[3-7].

In this study the specific type of modification utilised is plasma surface alloying, in the form of plasma nitriding, carburising and carbo-nitriding, following success in previous work[5, 8-12]. The effects of the above were examined on sample specimens, prior to application to a replica ice skate blade, with regards to surface and near surface hardness, wear resistance

and corrosion resistance. In service conditions have been replicated using synthetic ice, to simulate a real world situation.

Following completion of testing it has been possible to determine that through the application of surface modifications to materials such as stainless steels, which are used in a wide variety of applications, it is possible to improve the surface and near surface properties of the parent material without affect the base bulk properties of the substrate. Thus improving the tribological properties of the materials examined during the course of the study.

2 Literature Review

2.1 Ice Skating

2.1.1 Ice skating background, history and equipment

Ice skating is the process of sliding or travelling over an ice covered surface using a blade to aid the gliding process. Originally used as a method of transport, in Northern Europe and Scandinavia, where winters were long and the ground was frequently frozen, the oldest skate has been dated to around 3000 B.C[13, 14]. It was no more than a small piece of animal bone which could be tied to the foot using leather straps, figure 1. It has been demonstrated that through the application of this simple form of transport, 10% of the energy required for survival during the winter months could be saved, when compared with walking[15].

Figure 1 Replica of original bone blade attached to leather shoe with leather binding

As early as the early 1600's ice skating was introduced to the UK and several other countries, by both the Dutch and the Vikings. In the UK where winters were not severe enough to make ice skating a viable form of transport, it was more often used as a means of

entertainment, skating on frozen ponds and lakes. It is hypothesised that it is from here that the sport of figure skating draws its origins.

Figure skating, derives its name from the shapes or figures that are carved into the ice as the skater moves around, traditionally the image that represents this is a figure of eight. The sport as we recognise it today was the brainchild of an American called Jackson Haines, who in the 1860's popularised a new form of skating, whereby skaters dance and skate in time to music[16]. Initially as a sport it proved to be very popular in Europe, and after only 30 years or so in existence the first European and World Championships were held and a world governing body the ISU (International Skating Union) was established in 1892 in order to provide regulation for these events.

During the late 19th century organised events with standardised rules began to emerge, and by the 1920's it had developed into an Olympic sport[17]. Nowadays ice hockey is very popular in North American, Scandinavian and Eastern European countries, with elite leagues in these countries producing some of the world's best players. Athletes involved in these leagues earn large sums of money, with bonuses which are often performance based. Performance can be related to several factors, skill, fitness and equipment. With regards to the equipment, it is the technology and materials, and the engineering of these materials which can help to boost athlete performance levels.

Speed skating also owes much of its development, to the establishment of the ISU, the introduction of an international regulatory body, meant that worldwide arbitration could occur with regards to recording times over set metric distances[18]. Events are run over a large variety of distances, up to 10km, thus it is important that equipment is able to perform

consistently over the entirety of the race period[18, 19]. Examples of Olympic figure skating and speed skating can be seen in figure 2.

Figure 2 (a) Olympic Speed Skating, (b) Olympic figure Skating

2.1.2 Blade

From animal bone the next progression was to use a blade fashioned from wood, which was again attached to the foot, or boot. With both of these forms of skate sticks or poles were used to provide the required propulsive power for travel.

In the 14th century, in the Netherlands, an iron plate was inserted into the base of the wooden blade in order to try and reduce friction during sliding. From here the progression to a blade with sharpened edges followed in the early 1500's[17, 20], which removed the need to use poles as the primary form of propulsion, as the edge provided a stable platform to push from. In 1865, Jackson Haines attached a steel blade directly to a boot[20], creating the

first true example of the ice skate we know today. Nowadays ice skates come in three main varieties; (1) figure skates, (2) hockey skates and (3) speed skates.

With the evolution towards an edged sharpened blade, came new demands concerning edge angle and sharpness, which have great effect on turning circle and distance to come to rest. Greater control over these movements can be achieved by introducing a Radius of Hollow (ROH) into the blade-ice contact region as can be seen in table 1[21, 22].

Table 1 Typical Blade dimensions

Skate Type	Ice Contact Length (cm)	Blade Width (cm)	ROH (cm)
Figure Skate	20	0.35	1.10
Hockey Skate	22	0.35	0.95
Speed Skate	46	0.35	1.60

In general the smaller the Radius of Hollow (ROH) then the greater the sharpness which can be achieved in the ice contact surface. If a larger ROH is used then the gliding performance of the blade is increased, but a corresponding sacrifice in grip when turning and stopping occurs[23]. An example of a simple blade with dimensions can be seen in figure 3.

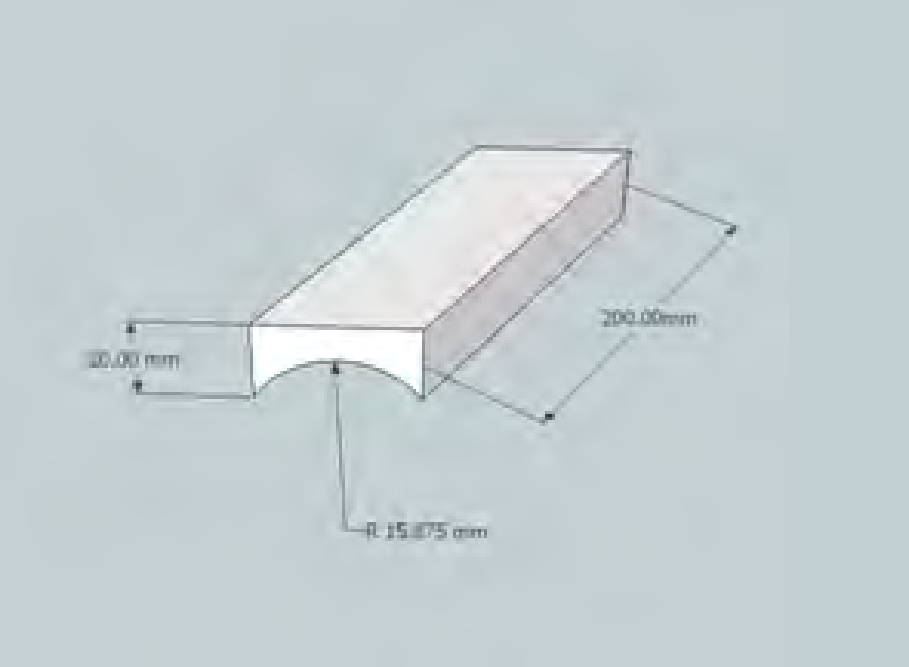

Figure 3 Basic ice skate blade design

The other design consideration when producing an ice skate blades is the curvature of the blade at either end, known as the rocker. This influences the turning circle of the blade, with the following relationship being established; the greater the curvature of the rocker then the smaller the corresponding turning circle of the blade[23]. In general a sharper turning circle is required for figure skating than for ice hockey or speed skating, owing the sharp turns and jumps that are required in this discipline.

3.1.3 Boot

Originally when blades were no more than a piece of bone or wood, then boots were equally as simple in so much as they were just the skaters usual footwear with the makeshift blade fastened to the sole.

Like when considering the design of the blades, each skating discipline has a slightly different design when considering the boot. Figure skaters tend to employ a boot, made of several layers of toughened leather stitched together in order to provide the required amount of support for the skaters ankle[24]. Ice Hockey and speed skating however, follow a slightly different design, where the leather "skin" is reinforced by either, moulded plastic or nylon, or a combination of the two[24].

When considering ice skating in its various disciplines as an elite performance sport, the motivation during the design process is to optimise equipment to allow athletes to perform to full potential. When considering each individual discipline there are requirements which are specific to each piece of equipment. For figure skating it is important that the skate provide sufficient support and stability, during the high speed spins and landings from jumps, to help reduce the risk of injury, and to provide the required stability for a smooth transition in to the next figure[1]. With ice hockey, potential sources of injury are similar to those seen in figure skating, the skate must be able to withstand the forces involved during rapid changes of direction, in addition it is essential that the skate be strong enough to withstand impact from sticks during the match. This means that whilst the skate must be light and manoeuvrable enough to not hinder performance in any way, is must also be tough enough to withstand the aforementioned impacts.

It is important to minimise the risk of exposure to injury, as high level athletes rely heavily on performance related bonuses from sponsors and teams to make a living. Thus if it is possible to prevent this through the use of technology and find a suitable engineering solution then it is beneficial to all parties involved.

Speed skating presents a different challenge to skate designers, as the skate is designed to maximise speed, through a combination of a smooth blade for gliding, and a good transfer of energy from push off. In order to maximise this recently a skate design known as the "clap" skate has begin to be introduced. The clap or clapper skate has a hinged blade which is not attached to the boot at the heel, it is suggested that this design serves to maximise power transfer during the skating motion, helping to boost performance. This is achieved by a longer contact time between the skate blade and the ice, which allows for a longer push off power phase[25, 26]. It has been shown that through the use of clap-skates in elite speed skating, performances have shown improvements of up to 5%, when compared with a traditional skate design, when considering both pure speed and times[27, 28]. The difference between a conventional skate and a clap skate can be seen in figure 4.

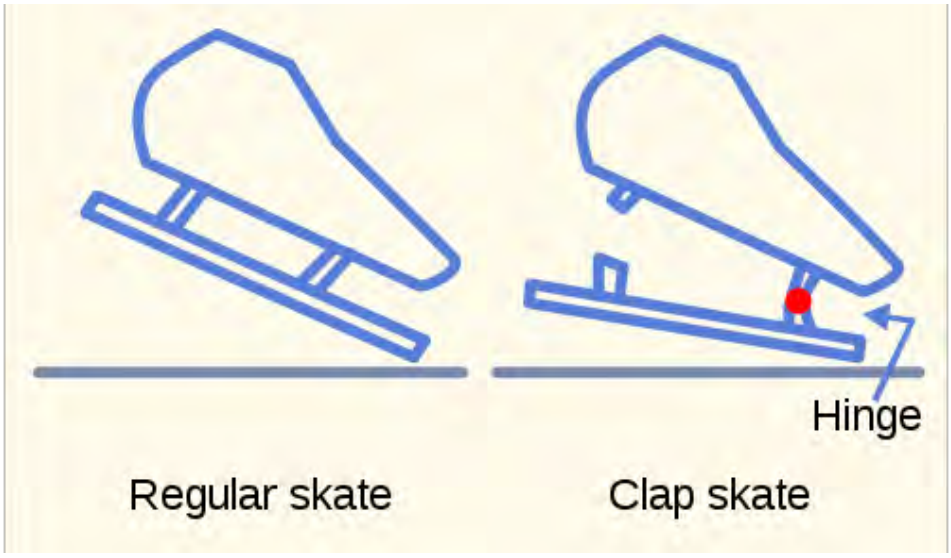

Figure 4 Comparison of regular fixed heel ice skate and hinged free heel clap skate for speed skating

2.1.4 In Service Requirements

Ice skating exposes equipment to a harsh in service environment, with several mechanisms operating which can result in damage to the equipment. The blade of the skate is exposed to high contact stresses when it comes into contact with the ice, thus the material must be of a sufficient hardness to prevent damage the surface of the blade. It is also essential for the chosen material to exhibit good wear resistant properties, as despite its low coefficient of friction, in the region of $\mu = 0.01$[29]. Ice sliding can still result in wear occurring. One study into ice friction during skating has suggested that as the speed of the skater increases then the coefficient of friction will increase accordingly[30], this could similarly be true for other winter sports applications such as skiing and bobsledding.

The true reason for the low coefficient of friction exhibited by ice is disputed between two main theories, that of pressure melting first described by Reynolds in 1901, and further examined during subsequent decades[31, 32] where the weight of a blade/edge pushing down on the ice results in the production of a thin layer of water which promotes a reduction in

friction. The second theory proposed by Bowden et al[2], is that of melting due to frictional heating, in this case frictional heat liberated from the sliding interface region, causes a rise in the surface temperature of the blade, which can lead to localised melting which produces a similar film of water which facilitates sliding motion[2]. This theory was examined in a further study by Colbeck et al[33], who determined that whilst pressure melting can make some contribution to reducing the friction experienced when sliding against ice, frictional heating is likely to be the main driving force. More recently it has been proposed that it is likely to be a combination of the two, resulting in a "mixed lubrication" mechanism[34].

Wear mechanisms which generally operate in the blade-ice interface region, occur as a result of the sliding motion of the blade over the ice. During ice skating, it is likely that the skate blade will experience a combination or types of wear, most commonly adhesive wear and melting/sliding wear.

Adhesive wear occurs when two bodies slide against one another, resulting in a transfer of material to one another. Small particles will be removed as a result of plastic deformation promoted by the sliding action[35], the size of the particles is dependent on the surface roughness of the individual bodies, as well as how hard the surfaces are. The lower the surface roughness of each surface, i.e the skate blade against ice, the lower the amount of friction and in turn wear that will be experienced. The removal of these small particles results in eventual breakdown and failure of the body in question.

It is also possible that a certain amount of abrasive wear may occur during the sliding process. Initially from simple ice contact, and further following melting of top layer of ice and formation of thin moisture layer. This will result in particles trapped within the ice being exposed, the implication of which is that these particles, will grind against the blade during

sliding, resulting in the removal of material from the blade surface[35]. Specific studies regarding abrasive wear in winter sports situations have been carried out by Ducret *et al*.[36], whom have observed that the severity of the wear experienced, is dependent on the contact angle with the ice and snow.

When considering the performance of the blade the above are very important, as during the initial contact phase with the ice, when impacting, both blade sharpness and roughness are affected. This can result in a loss of efficiency during the push off phase, as the blade sharpness decreases the efficiency with which energy is transferred from potential to kinetic is greatly reduced. Sliding efficiency is further decreased as a result of increased surface roughness due to exposure to wear mechanisms; resulting in a rise in the amount of friction experienced, thus reducing performance of the blade.

2.1.5 Current Materials

Currently there are two main materials used in the manufacture of ice skate blades, these are carbon steels and austenitic grades of stainless steels. Traditionally carbon-steel blades are coated using a hard chrome plate, and are preferred to the austenitic grade steels for cost purposes. Increasingly a third option is being introduced which is to create the majority of the blade from a single extruded piece of aluminium, with a steel runner mounted and fastened to provide the contact surface with the ice. This third option has been promoted largely by Paramount skates, with steel insert blades being produced from martensitic grades 420/440. Another possible option is the use of a plastic body, with a steel insert as the runner in contact with the ice.

Each of these approaches has its benefits, and can be employed based on the demands of the consumer to produce the required specifications. When approaching a design based purely on cost, then the preferred option is to choose the carbon steel approach, as it is cheaper to obtain and manufacture. However, when considering a performance based approach, the better option is to utilise a blade containing stainless steels. By using stainless steels the blade remains sharper for a longer period of time, as they are naturally harder than carbon steels; the blade is also more resistant to corrosion and rusting due to the passive/corrosion resistant properties exhibited by stainless steels. This means that the lifetime of the blade is improved through improved resistance to sudden failure due to flaws introduced as a result of corrosive attack. Whilst there is a slight weight difference in stainless and carbon steels, it is likely that this can be accounted for during the design process of blades.

Manufacturers of the paramount blades claim that by using stainless steel as the runner on the blade time between blade re-sharpening can be increased by between 80 and 120 hours[37]. It is possible to further improve the potential performance of an ice skate, through the use of an aluminium framework for the blade with a stainless steel runner; this can reduce the weight of the blade by up to 50%. The framework is composed of milled aluminium, and the construction of a blade composed of this construction can be seen in figure, this is a typical combination blade fabricated by Paramount Blades, seen in figure 5 .

Figure 5 Paramount combined blade design, with Aluminium framework and a stainless steel runner for contact with ice

The steels used for these runners are annealed martensitic and duplex grades, which have been hardened through quenching. When looking specifically at Paramount blades, the steels used are 420C and 440C grades[38].

A comparison of the current materials used during the manufacture of ice skate blades can be seen in table 2.

Table 2 Typical ice skate blade materials, summary

Material	Positives	Negatives
Carbon Steels	Cheaper to produce	Reduced durability and corrosion resistance
Stainless Steels	Durable, Corrosion Resistant	More costly to produce
Aluminium + Stainless Steels	Durable, Corrosion resistant, lightweight	Relatively expensive to produce

2.2 Materials Data

2.2.1 Stainless Steels Introduction

Stainless steels are a range of materials which are used on a daily basis in any number of vital applications, including; construction, industrial, medical, automotive, aeronautic,

cryogenic and sporting. In 1905, it was discovered that steels with a Cr content in excess of 9% exhibited acid resistant properties, which initially led to their use in rifle barrels in order to attempt to lessen the effect of erosion[39]. Stainless steels are available for use in such a wide variety of different potential applications due to the properties exhibited by the various grades of stainless steels, such as excellent corrosion resistance, and the ability to retain properties in both high and low temperature environments. Grades of stainless steel whilst all exhibiting the same basic composition (with regard to the presence of Cr), each have different specific properties, with regards to hardness, wear resistance and corrosion resistance.

The basic composition of this group of materials is a Fe, Cr, Ni based alloy, whereby the ratios of these three base elements determine the properties specific to each grade of steel. In austenitic stainless steels for example, a common composition might be 16%Cr, 6% Ni, with Fe making up the majority of the rest of the sample. In the case of austenitic steels it is also possible to add various elements to the alloy such as, Mo, Ti or Cu, in order to modify or improve properties[40]. However, currently these steels are not applied in ice skating applications.

Another form of stainless steels is the martensitic family, in this case the major alloying element is also Cr but it is common for them to retain a higher C content than the other groups, and no Ni. The other common “families” of stainless steels include; ferritic, duplex and precipitation hardened[41]. As discussed previously, these steels are currently employed in skate blades.

Although on the whole stainless steels possess excellent resistance to corrosion, one potential drawback, and problem in terms of certain applications, is the tendency of austenitic stainless steels to exhibit poor wear resistance and low hardness.

For the purposes of this study the focus will be on the austenitic and martensitic families of stainless steels. As austenitic stainless steels, account for almost 70% of the total market sales of stainless steels[42], and relatively small numbers of studies have been carried out on martensitic stainless steels, and due to their naturally higher hardness they promote themselves as a potential candidate for use in ice skating applications.

When considering martensitic stainless steels the following general properties can be established; on the whole martensitic samples will be, composed of 11-13% Cr, they will be ferromagnetic (medium), hardenable through heat treatment[40, 43], show good corrosion resistance, low ductility, low weldability, and only exhibit mediocre resistance to applications in conditions where they may be exposed to temperature extremes[40]. When considering their resistance to corrosion the major they are their optimum performance in applications where atmospheric corrosion is the predominant mechanism[42]. Another difference that martensitic samples exhibit when compared with ferritic and austenitic samples, is the much higher C content which is shown, which in some martensitic grades can exceed 1%, whereas in many austenitic and ferritic steels it can lower than 0.03%[44]. The Carbon content present in the Martensitic grades is very important because it can help to determine the wear resistance which may be exhibited by a particular sample[42].

Martensitic stainless steel differs from Austenitic steel by the fact that it naturally exhibits higher hardness values in the material surface. This occurs as a result of the way in which martensitic stainless steel is formed. In order to produce the martensitic effect, austenitic

samples are heated, then rapidly cooled (quenched), in order to prevent the formation of a ferritic stage. This quenching promotes a phase transformation, from the parent austenite, and is exhibited in the crystal structure shown by martensitic samples[41, 45]. Due to its brittle nature, it will normally require further tempering in order to permit the diffusion of C present in the material, away from the surface layer[46].

The phase transformation which occurs results in a change in the crystal structure exhibited in the material, in a martensitic grade the crystal structure will primarily be Base-Centered-Tetrahedral (BCT) as opposed to the Face-Centered-Cubic (FCC) structure exhibited in the austenitic family, or the Base-Centred-Cubic (BCC) structure exhibited in the ferritic family[42, 43]. The extent to which phase transformation occurs is dependent on temperature. That is to say that martensite formation proactively occurs within a clearly defined temperature range, between the Martensite start (M_s) and the Martensite Finish (M_F) temperature[43] which is dependent on the specific grade.

When considering austenitic grades it is useful to note that both martensitic and ferritic grades can be formed from austenitic parent grades. This is done through cooling processes, either through slow cooling (forming ferrite) or rapid quenching (forming martensite).

2.2.2 Applications

Stainless steels are involved in an incredibly wide variety of applications which ranges from construction and industrial, through to automotive, aerospace and sporting. When considering construction and industrial applications properties involving strength are important, and stainless steels are often used as internal support structures in buildings. In the automotive industry stainless steels are often chosen as a result of their ability to

perform in a crash situation. It is possible in such a situation for the steels to improve their hardness by up to 4 times the original value[42], due to the phenomenon known as work hardening. Although stainless steels are of a higher density than other materials used in automotive industries, their strength to weight ratio is comparable to many other materials utilised, such as aluminium and titanium alloys, they are a popular choice for many components.

Due to their excellent resistance to acid attack, stainless steels find an application in the aerospace and aviation industries, where they are used for turbines, jet propulsion units and in addition often comprise large portions of the structural framework. They are also involved in many domestic applications such as in cookware, crockery and many tools that are found in almost every home.

In sporting applications equipment is often exposed to a combination of temperature extremes and highly corrosive environments. This makes stainless steels the logical choice for equipment such as, alpine ski edges, ice skate blades, luge and bobsled runners, in auto sports and in many exercise machines commonly found in gymnasiums. Stainless steels also find many applications in the automotive industry as components in cars, motorbikes and boats. Examples of some typical applications of stainless steels can be seen in figure 6.

Figure 6 Examples of general applications of stainless steels, (a) blades from motor boat propeller, http://www.bartswatersports.com/images/product/largeimage-7521.jpg, (b) Esspresso machine, http://sale.images.woot.com/Breville_BES400XL_Ikon_Espresso_Machine_930Detail.jpg

2.2.3 Properties of selected grades for study

For the study in question the grades of steel chosen, were High Nitrogen AISI 316 (austenitic) Stainless Steel, and AISI 420 grade (martensitic) Stainless Steel.

In general martensitic steels, such as (AISI 420) are optimised for high hardness, at the cost of a reduction in performance of properties such as corrosion resistance; they also exhibit a potential loss of ductile behaviour at sub-zero temperatures. They are also somewhat limited in high temperature applications, above the tempering temperature, owing to a potential reduction in mechanical properties. Despite this, AISI 420 grade makes a good choice for applications at relatively low temperature in the presence of a mildly corrosive environment[47].

2.2.4 Problems

In application, austenitic stainless steels suffer several potential constraints, which are related to issues which may arise as a result of their specific properties. Despite their many excellent properties such as resistance to corrosive environments and high tensile strength and good modulus of elasticity, stainless steels can be susceptible to failure. Commonly problems that occur are related to tribological issues, which is to say situations or applications where stainless steels are exposed to environments in which their hardness and wear properties are brought into requirement It has been well documented that stainless steels, have relatively poor hardness and wear properties which can lead to them failing in service[48, 49]. Tribology is defined as the science of friction, lubrication and wear concerning interacting surfaces in relative motion[50, 51]. Advances in this domain have resulted not only in vast improvements in performance, but also in the saving of millions in industrial applications[50].

When considering ice skate blades they are exposed to a combination of wear mechanisms, the most prominent being adhesive wear. Brought about through sliding contact with ice and any impurities contained therein.

These poor tribological properties, can also lead to in service failure largely owing to the breakdown of the protective oxide layer observed in stainless steels, which promotes their resistance to corrosive attack. If the breakdown of passivity does occur then the main body of the steel becomes vulnerable to corrosive attack, which can occur in several forms; crevice, pitting, and inter-granular, being the most common. When considering ice skate blades the most dominant form of corrosion is likely to be pitting corrosion. Each form of

corrosive attack occurs as a result of a different mechanism which is dependent on both the materials present, and the environment in which they are operating.

Pitting corrosion occurs on a localised scale, where small holes or pits form on the surface of the metal. It comes about due to de-passivation of small regions of the surface oxide film, as a result of chemical or mechanical damage[52]. The region in the interior of the pit becomes anodic as a result of oxygen starvation, thus the aerated region at the surface forms as a cathode, and material is transferred and deposited. Pitting corrosion is often considered to be one of the more dangerous forms of corrosion, as it occurs in an unpredictable pattern, and is very difficult to detect. Furthermore pitting corrosion can serve to result in a rise in local stresses.

This may be especially important in an application such as ice skating, where steel blades are exposed, to an environment which results in attack from contact stresses, wear mechanisms and a mildly corrosive environment. When considering ice skating, and potential corrosive attack, it is important to consider several factors. Whilst with indoor rinks it is possible to retain a reasonable amount of control over the specific chemical composition, in outdoor rinks, there is a greater possibility for variation due to the influence of environmental factors.

2.3 Solutions

2.3.1 Solutions

It has long been possible to alter the inherent properties of a material in order to improve the desired properties[53]. This has been evident through history, in the improvements seen in not only tools, but weaponry, transport and building materials. It is possible to improve

the poor tribological properties exhibited by SS, thus making them a viable choice for a wider variety of applications. Improvements with regards to the tribological properties of steels and stainless steels, have been known of for several centuries and is this time much work has gone into determining the most effective methods to achieve the desired results[53]. Improvements can be achieved using several different techniques, the most simple, being to use a martensitic stainless steel with appropriate heat treatment.

However, it is possible to achieve much greater improvements through the application of surface engineering (SE) technologies[53]. Involving either the application of a coating to the parent substrate, or by modifying the surface and near surface region of said substrate.

Common surface coating methods employed with stainless steels are Physical Vapour Deposition (PVD) and Chemical Vapour Deposition(CVD)[9]. Other coating methods include techniques such as thermal spraying. Whilst these coating methods certainly improve both resistance to wear and hardness, as well as reducing roughness and friction, the deposited layer is relatively thin, and depending on the quality of the bonding between coating and substrate can be relatively easily removed during application. Presenting the problem in an application such as ice skating, where the stainless steel blade is exposed to repeated impact against ice, which is likely to break through the coating relatively rapidly. As a result of this in order to achieve the desired improvement in the properties of the parent grade it is necessary to turn to other options.

Surface modifications prove a better option as the technique does not simply coat the substrate but interacts with the substrate on a molecular level, creating a greater level of interaction. In the case of surface modifications, it is not simply the surface which is altered; it is the entire near surface region of the bulk parent material. The result is a layer of

modified substrate which shows improvements identical to those seen on the modified surface, without any effect being had on the properties of the bulk of the material.

Surface modification encompasses a variety of techniques, which help to promote diffusion of ions through the near surface region to produce the modified layer. Common techniques used are ion implantation, traditional nitriding and carburising treatments, Plasma Immersion Ion Implantation (PI^3) and Plasma assisted surface modification. Whilst all of these methods work on the same principles, that is to say introducing a new atomic species into the near surface region[53-55], each proves effective in a different manner, with its own specific set of negative and positive elements.

Ion implantation methods are based on the surface of the substrate being bombarded with a focused accelerated ionic beam[54]. Traditional ion implantation is a line of sight treatment, whilst PI^3 involves immersion of the substrate in a low pressure plasma field[56], this ensures that all exposed surfaces can be exposed to the treatment simultaneously[5]. Immersion in the plasma also helps to increase the amount of energy with which the ions contact the surface of the substrate, which promotes deeper diffusion into the parent material. Studies have shown that the modified layer produced using the PI^3 techniques exhibits improved tribological properties due to the high nitrogen content found in the modified supersaturated near surface region[56].

Traditional nitriding and carburising treatments (thermo-chemical treatments) are conventionally either as solid, liquid or gaseous methods. Where carbides or nitrides are precipitated into the sample in a medium which is heavy in either Nitrogen or Carbon, allowing diffusion into the sample surface. Solid and liquid state treatments are almost never used currently, and traditional gas methods have more recently been replaced with a

move towards plasma assisted surface modification[10, 57]. Through the use of plasma during the treatment process the energy with which the charged ions bombard the surface is greatly increased. During the treatment process the substrate surface is sputtered with charged ions, which force their way into the interstitial spaces in the atomic lattice of the basic substrate. In traditional methods, samples are heated to temperatures in the region of 800^{o}C, whereas in plasma assisted modification treatment temperature rarely exceeds 500^{o}C[12, 58]. There are several methods of Plasma assisted nitriding and carburising, most commonly used are either DC or Active screen. Active screen treatments possess the added benefit of being able to be carried out on non-conductive materials such as polymers.

Plasma thermo-chemical and PI^3 modifications produce, a modified layer which is similar in hardness, and corrosion resistance[5], but nitridng and carburising offer several benefits over other methods of surface engineering. Most prominent is the fact that these techniques are capable of producing consistent and reproducible results, owing to the control which can be achieved over treatment conditions and the resulting nitride layer.

2.3.2 Low Temperature Plasma Surface Alloying (LTPSA)

Low temperature plasma surface modifications offer a number of benefits when compared with more traditional high temperature methods, and have been increasingly preferred over the past couple of decades[59]. Perhaps most notably, it has been established that by carrying out modification at low temperature, issues related to a loss of corrosion resistance associated with high temperature treatments are avoided. This is due to the prevention of the formation of precipitates in the modified layer which are seen in treatments at more traditional temperatures. Precipitates which form in the modified layer, are chromium nitrides and carbides, depending on whether nitriding or carburising modifications are

applied, resulting in depletion of the chromium content in the parent substrate occurs, which in turn results in an associated loss in corrosion resistance[60]. Low temperature treatment offers several other benefits over more traditional higher temperature options. Treating at lower temperature helps to prevent dislocations in the substrate matrix during cooling, which can lead to the presence of damaging residual stresses. Low temperature treatments can also help to reduce the presence of precipitates in the treated region. Additional benefits of using LTPSA, as compared to older technologies for these processes are a reduction in energy consumption, during treatment process, reduction in the quantities of any harmful or toxic by-products, such as greenhouse gases[53].

There are however, some disadvantages to the use of LTPSA. Treatment times are generally more prolonged as the lower treatment temperature serves to slow the diffusion rate of the alloying species into the parent substrate. From this it is often seen that lower temperature treatments do not exhibit the same modified layer depths as those shown by the more traditional choice of treatment temperature.

Low temperature plasma modification is generally a gaseous technique, which has been developed to maximise the aforementioned benefits. Parent substrates are exposed to a cold gas plasma, known as glow discharge, consisting of ionised gas molecules[61]. Gas is ionised by applying a current during the alloying process, the ions produced are used to sputter the surface of the parent substrate. During the sputtering process, the charged gas ions bombard the substrate surface, and force their way into the interstitial spaces between the atoms in the parent matrix. Low temperature plasma modification is surface specific and thus can be used to alter the surface and near surface region of a sample, without affecting the bulk properties.

2.2.3 S-Phase

Following plasma surface alloying, improvements to the wear resistance and hardness of stainless steels, has been widely documented in previous studies[5-7, 11, 47, 48, 62]. It has been proposed that this is due to the formation of a modified surface layer known most commonly as an "S-phase" region. It has also been referred to as "m-phase" and γ-N[63]. This region not only exhibits improvements in the tribological properties of stainless steels, but can in treatments carried out at relatively low temperature <500^{o}C, also retain the corrosion resistant properties, which during high temperature treatments are often damaged due to the formation of precipitates[55], as described previously.

Presence of the S-phase region in austenitic stainless steels (ASS) has been examined, with regards to the benefits to wear resistance and hardness, in a number of studies [3, 12, 48, 55, 64, 65], however, significantly less emphasis has been placed on the study of martensitic steels. With regards to the "s-phase" region in austenitic stainless steels, it is observed as a region of expanded supersaturated austenite, exhibiting a face-centred-cubic (FCC) or face-centred-tetragonal (FCT) crystal structure [55, 63, 66]. "S-Phase" region is generally observed as being featureless and precipitate free, following low temperature plasma treatments. However, once treatment temperature rises above ~500^{o}C the formation of CrN precipitates is observed, during nitrding[66]. It has been suggested that it is the formation of these precipitates which leads to an associated reduction in resistance to corrosion [55, 64, 66].

In ASS it is suggested that the formation of this "S-phase" region occurs as a result of diffusion of charged gas ions into the surface and near surface region of the parent substrate. The Nitrogen occupies interstitial gaps within the atoms of the parent matrix, resulting a in a subsequent expansion in the crystal lattice. It is from this expansion that the

term “expanded austenite” has been coined, it can be observed using a variety of characterisation methods. When considering XRD, it is seen as a shift in the 2θ diffraction angle, using microscopy it is seen as a smooth bright layer, which is free from precipitates.

It has been proposed that it is this expansion of the lattice during the alloying process and the subsequent contraction during cooling leads to the formation of residual stresses in the surface and near surface region. It is thought that these residual stresses help to contribute to the improved wear resistance and hardness of the substrate material.

In martensitic stainless steels (MSS) the nitrogen enriched region is observed as a compound layer of the parent substrate with precipitates. The compound layer in MSS is formed in the same manner as with the S-phase region in ASS, with the ions diffusing through the parent matrix to form the modified layer. However, it has been observed that in MSS this occurs as a result of precipitation diffusion, and can be observed under microscopic characterisation of the compound layer [67-69]. Studies have suggested that the precipitates observed in the diffusion zone are likely to be γ’-Fe_4N, ε$Fe_{2-3}N$ and CrN nitrides [49, 67-69].

When making a comparison between plasma nitriding and plasma carburising, it has been established that there are certain fundamental differences in the effectiveness of each of the specific layers. Previous studies have shown that in nitriding treatments there is a greater improvement in there hardness of the surface and near surface region than in carburised layers. However, carburising produces a greater diffusion depth of the modified layer, than is the case with nitriding[70].

Furthermore studies[71] have shown that modified layers created using plasma nitriding can also help to improve resistance to hydrogen embrittlement. This helps to reduce the possibility of sudden catastrophic failure.

It has been shown that it is possible to generate both a nitrogen and carbon, S-phase on a scale sufficient to make it an increasingly utilised industrial method. More recently it has been discovered that it is possible to simultaneously produce a nitrided and a carburised layer. This form of surface modification is known as carbo-nitriding when the diffusion occurs into austenite, as with austenitic stainless steels. It is also referred to nitro-carburising, in ferritic substrates, where the compound layer is altered from the normal Fe_4N to (ε-$Fe_{2\text{-}3}$ (N,C)), exhibiting a hexagonal close packed (HCP) structure[8].

Nowadays studies have begun to investigate the formation of a boron S-phase however this is still very much in the developmental stage[10].

When considering plasma nitriding (PN), plasma carburising (PC) and plasma carbo-nitriding (PCN); it has been observed that treatment time, temperature and pressure can influence the effectiveness of the modified layer. By increasing treatment temperature it is possible to achieve a deeper diffusion depth for both PN and PC, however this results in the formation of precipitates within the S-phase region. As a result of increasing treatment time it is also possible to improve diffusion depth, into the parent substrate; however, this results in a substantial extra cost and is sometimes considered to be impractical.

3 Methodology

3.1 Materials and Specimens

Materials chosen for the study were typical grades of stainless steel which are either currently used, or plan to be used in the blades of ice skates, and the edges of skis. Grades chosen were AISI 316 (austenitic stainless steel) and AISI 420 (martentsitic stainless steel). The respective compositions of the materials chosen for the study are seen in table 3.

Table 3 Chemical composition of chosen stainless steels

		C	Cr	Ni	Mo	Mn	Si	P	S	Fe
AISI 316	ASS	0.08	17	12	2.5	2	1	0.045	0.03	Bal.
AISI 420	MSS	0.15	13			1	1	0.03		Bal.

AISI 316 used in the study is as received rolled steel, in bar form, cut into disc's. Discs were cut to the following dimensions: Φ=25mm, depth=5mm, giving a sample surface area of 13.75cm^2. AISI 420 used in the study was heated to 1130^{o}C for a period of 30 minutes, before being quenched in oil and tempered at 250^{o}C for a further 2 hours. Again disc samples were cut to the same dimensions as those for the AISI 316 samples. Disc samples were used to establish optimum treatment conditions, for nitriding and carburising to be used for the dummy blades in simulation testing.

For simulation testing replica blades were designed which allowed testing to be carried out to determine the effect of surface modification of the blade with regards to its hardness and tribological properties, with a view to improving performance and lifetime of the skate blade.

3.2 Surface Treatments

Once cutting of the discs had been completed, specimens were prepared for plasma surface alloying treatment. Prior to being placed in the plasma furnace, specimens were cleaned in an ultrasonic cleaner, initially in water for a period of 10minutes, and subsequently in acetone for a further 10 minutes. Following cleaning samples were introduced into the plasma gas furnace in preparation for treatment.

Treatments were carried out in a conventional 40kW Klöckner DC plasma unit, under a range of temperatures to provide a baseline from which to determine optimum conditions for subsequent modifications of dummy blade samples. Gas composition and treatment time were kept as a constant for the nitriding, carburising and carbo-nitriding modifications, to allow the effect of treatment temperature to be established. All treatments were carried out for a period of 15 hours, over a range of temperatures from 400^{o}C to 550^{o}C. A full summary of treatment conditions can be found in table 4, and a schematic of the set up of the plasma furnace used for the treatments can be seen in figure 7.

Table 4 Initial treatment conditions for sample disc specimens

Treatment	Time (hours)	Temperature (^{o}C)	Gas Composition
Nitriding (PN)	15	400, 450, 500	25% N_2 / 75% H_2
Carburising (PC)		450, 500, 550	2% CH_4 / 98% H_2
Carbo-Nitriding (PC-N)		400, 450, 500	25% N / 2% CH_4 / 73% H_2

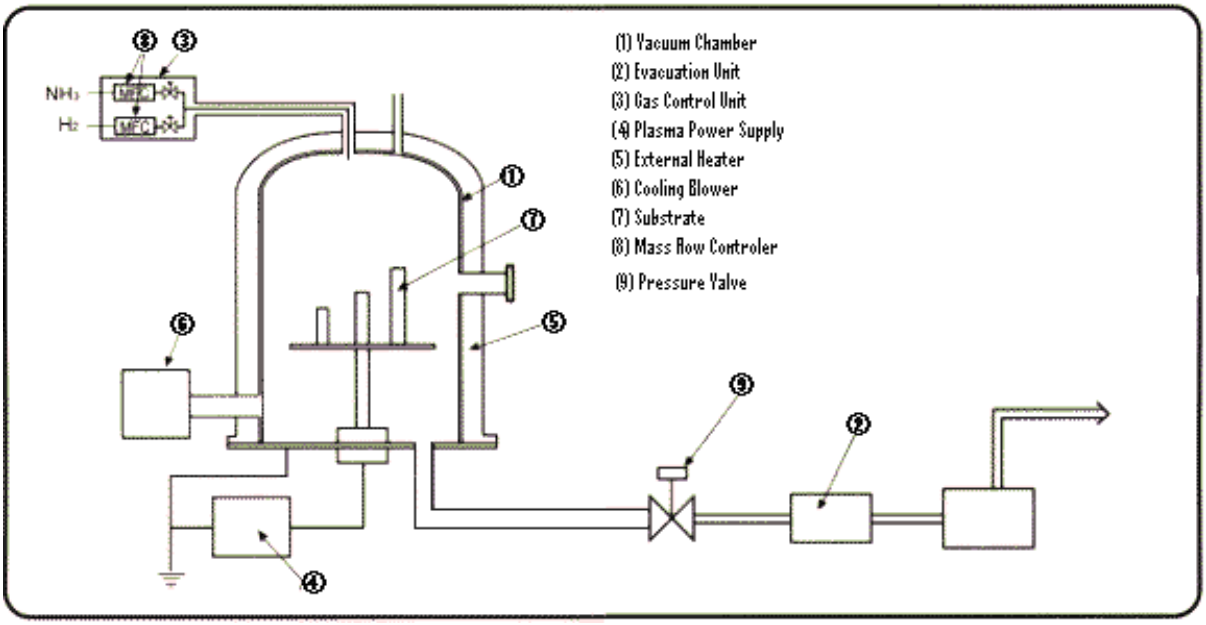

Figure 7 Schematic of Plasma Alloying furnace

During treatment specimens are placed on a platform within the centre of the furnace, the furnace is then pumped down to achieve a vacuum in the treatment chamber. Once a vacuum has been achieved the pressure within the chamber is set to 4 Mbar, for the entirety of the treatment process. Once the pre-set pressure has been achieved, a current is passed through the chamber, with the chamber wall acting as the anode and the specimen surface as the cathode. This allows a charged plasma field to be generated within the chamber. This plasma field within the furnace serves to ionise treatment gas upon its introduction to the treatment chamber. Depending on the form of treatment, nitriding, caburising or carbo-nitriding, either N_2, CH_4 or a combination of both, respectively, are introduced into the chamber, in the presence of H_2, which acts as a stabiliser. Once gas the gas has been introduced into the chamber, and has been ionised air is forced into the chamber to aid the flow of charged gas ions towards the surface of the specimen. Upon contact with the specimen surface, ions begin to force their way into the interstitial spaces in the parent atomic matrix.

Following treatment, cross-sectional samples of each of the specimens were cut in order to allow for measurements to be taken. Cross-sectional samples were mounted in bakerlite, prior to preparation for metallographic examination.

3.3 General Characterisation

3.3.1 Sample Preparation

Prior to further characterisation, samples were ground to 1200grit using wet and dry paper before being polished to a 1µm finish ready for hardness testing. Following hardness testing, samples were etched to allow micro-structural characterisation. ASS samples were etched in a 50%HCl / 50%HNO_3 for 20-30seconds or until mirror like appearance of surface becomes cloudy. MSS samples were etched in Kallings 2 Reagent (10mgCuCl/50ml HCl/50ml ethanol) for a period of 30seconds or until mirror like finish begins to fade. By etching the samples the microstructure of the specimen surface is exposed.

3.3.2 Optical Microscopy

Samples were examined at relatively low magnification, using optical microscopy. Both surface and cross-sectional views were considered in order to characterise differences between the treated and untreated samples. Samples were examined using a Zeiss Axioskop 2000, capable of imaging at magnifications of up to 1000x.

3.3.3 SEM

SEM examination of micro-structure, allows for images to be taken at higher magnification, with a higher resolution image obtainable[72-74]. Characterisation was carried out on a Phillips-XL30 SEM, images were obtained using a Secondary Electron (SE) detector. The

working distance (WD) used was set at 10, and a 20 keV acceleration voltage set for all metallic samples, and for synthetic ice samples the acceleration voltage used was 6keV.

Chemical compositional analysis was carried out using EDX characterisation. Allowing for the chemical structure of the parent substrate and that of the modified layer following treatment.

Examination was carried out following corrosion testing to attempt to determine the mechanisms of corrosion acting on the samples, pre and post treatment. Examination was also carried out following wear testing in order to characterise the wear mechanisms produced on the samples in their untreated and treated states.

3.4 Measurement

3.4.1 Chemical Analysis

Following treatment; Glow Discharge Spectroscopy (GDOES) was carried out on both the sample discs and the replica blades. GDOES is used to analyse the chemical composition of a sample as a function of depth from the sample surface. Analysis was carried out using a LECO GDS-750 QDP GDEOS machine, calibrated to normalise the composition of all elements present in stainless from values of 1 to 100% by atomic weight %. Special attention has been paid to the calibration regarding nitrogen and carbon composition, to determine the effects of treatment temperature, and type. Depth profiling was carried out for a period of 900 seconds, the integration time. Signals are recorded over this period, before being divided by the integration time in order to obtain the average signal.

Samples are placed in the spectrometer, and must cover the vacuum o-ring to ensure the best possible airtight seal. A plasma discharge is generated in order to sputter the sample

surface removing layers of the substrate to create a depth profile. The particles emitted from the sample surface are measured using an optical spectrometer which records the wavelengths of the particles which are emitted.

Data obtained is represented in graphical form as a function of concentration (at %), against depth (µm).

3.4.2 Hardness

Disc samples were subjected to both surface hardness testing and to cross-sectional hardness examination using a Vickers indenter and a Knoop indenter, respectively. Surface hardness was examined to determine improvement in resistance to contact stresses, attack from wear mechanisms, and a potential reduction in friction upon contact. Cross-sectional hardness examination was used to determine the effective depth of the treated layer, and to provide a comparison to the chemical composition depth profiles generated in GDS characterisation.

Surface hardness was examined using a Vicker's hardness indenter. In this instance a loading of $HV_{0.1}$ was applied to the sample surface for a period of 10seconds using a diamond tipped indenter.

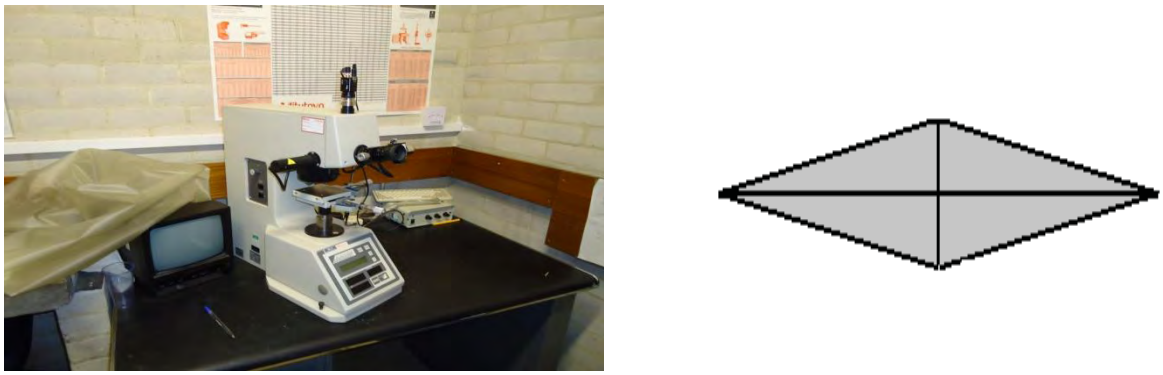

Figure 8 - (a) Matusoyo Micro-Hardness indenter, (b) Knoop indent

Cross sectional hardness was examined using a Knoop micro-hardness test, a loading of 98.07N is applied to the sample surface for 10 seconds. The indenter is in the shape of an elongated diamond, as seen in figure 8, further information regarding knoop micro-hardness analysis can be found in a previous study, by Hays and Kendall[75]. It is possible to calculate the knoop micro-hardness value using equation 1.

Equation 1 - Knoop Microhardness $$HK = \frac{Load(kgf)}{Impression\ Area\ of\ Indentation\ (mm^2)} = \frac{P}{CL^2}$$

Where: HK=Knoop Hardness (N/m^2) C = Indenter Constant (0.070)

P = Load (N) L = Length of Long Diagonal (m)

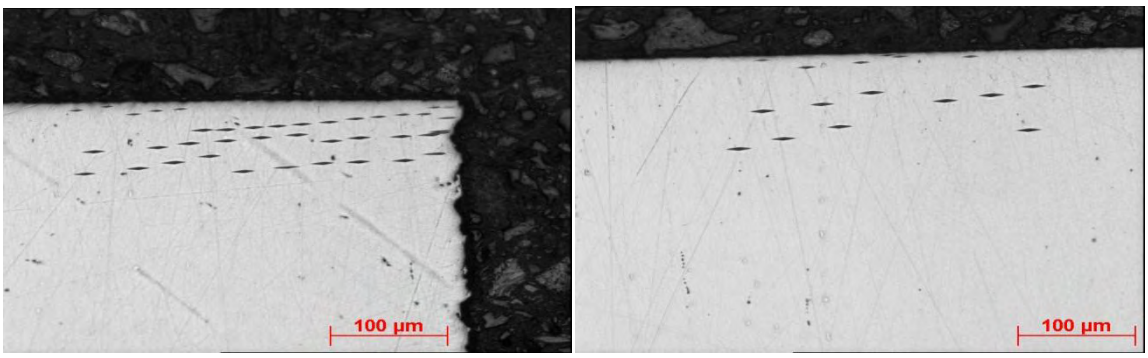

Figure 9 – Knoop Micro-Hardness indent measurements for cross-section micro-hardness measurements

3.4.3 Corrosion

Corrosion testing was based on immersion testing carried out in a study by Li and Bell, where samples are immersed in a 3.5 % NaCl solution to simulate a marine environment[65]. This solution was created by mixing de-ionised H_2O with pure NaCl crystals. This simulates

corrosive environments to which stainless steels are often exposed during service, as well as representing a worst case in service scenario for ice skate blades. Samples were weighed before immersion, after 72 hours and after a further 120 hours, from the weight loss values obtained it was possible to calculate the corrosion rate (µm./year). Corrosion rate was calculated using equation 2.

Equation 1 – Corrosion Rate $$\boldsymbol{Rate\ of\ corrosion = \frac{K \times \Delta m}{A \times T \times D}}$$

Where:

K = Constant, for µm/year, 8.76×10^7 Δm = Mass loss (g)

A = Exposed Area (cm^3) T = Exposure time (hours) D = Density (g/cm^3)

3.5 Synthetic Simulation Testing

3.5.1 Blade Design

Following completion of analysis of sample discs, dummy blades were designed to replicate the contact surface of a true ice skate blade. These dummy blades were subsequently treated according to the optimum treatment conditions established during characterisation of the sample discs. Dummy blades were designed according the following specifications; length=240 mm, width=3.81 mm, height=20 mm. Radius of Hollow selected for the blades was 15.875 mm, thus the blade represents halfway ground between a figure skate blade and an ice hockey blade. Prior to treatment blades surfaces were prepared by being rubbed with 1200 grit wet and dry paper, before cleaning in acetone in an ultrasonic cleaner for a period of 10 minutes.

Following establishment of the optimum treatment conditions based on results obtained from the analysis of sample discs, the treatment conditions outlined in table 4, were used

for the surface modification treatments of the dummy blades. Following completion of the treatments blades were cut to produce scale test pieces, for simulation testing. Test pieces were cut to length=20 mm, width=3.81 mm, height=20 mm, using a bonded silicon-carbide cutting wheel.

Table 5 Treatment Conditions for replica blades

Treatment	Time (hours)	Temperature (^{o}C)	Gas Composition
Nitriding (PN)	15	450	25%N_2/75%H_2
Carburising (PC)	15	500	2% CH_4 / 98% H_2

3.5.2 Synthetic Ice

For the purposes of simulation testing, a synthetic ice counter face has been produced for wear testing of untreated and treated dummy blades. Synthetic ice is constituted of a Polypropylene (PP) matrix with Silica (SiO_2) particles introduced to replicate particles which are found in naturally occurring ice. The composition of the counter face material is 75%PP and 25 % SiO_2. It was formed, by melting the PP down to form a crepe, before $Si0_2$ particles were added, the crepe was then placed in a mould, before being placed into a hydraulic press maintained at 10Mbar during cooling. A complete sheet of the synthetic ice counterpart can be seen in figure 10. Distribution of the SiO_2 particulates can be seen in figure 10 (b) under optical microscopy. Surface and cross-sectional views of the polymer matrix can be seen in figure 10 (c) and (d) respectively, using SEM characterisation.

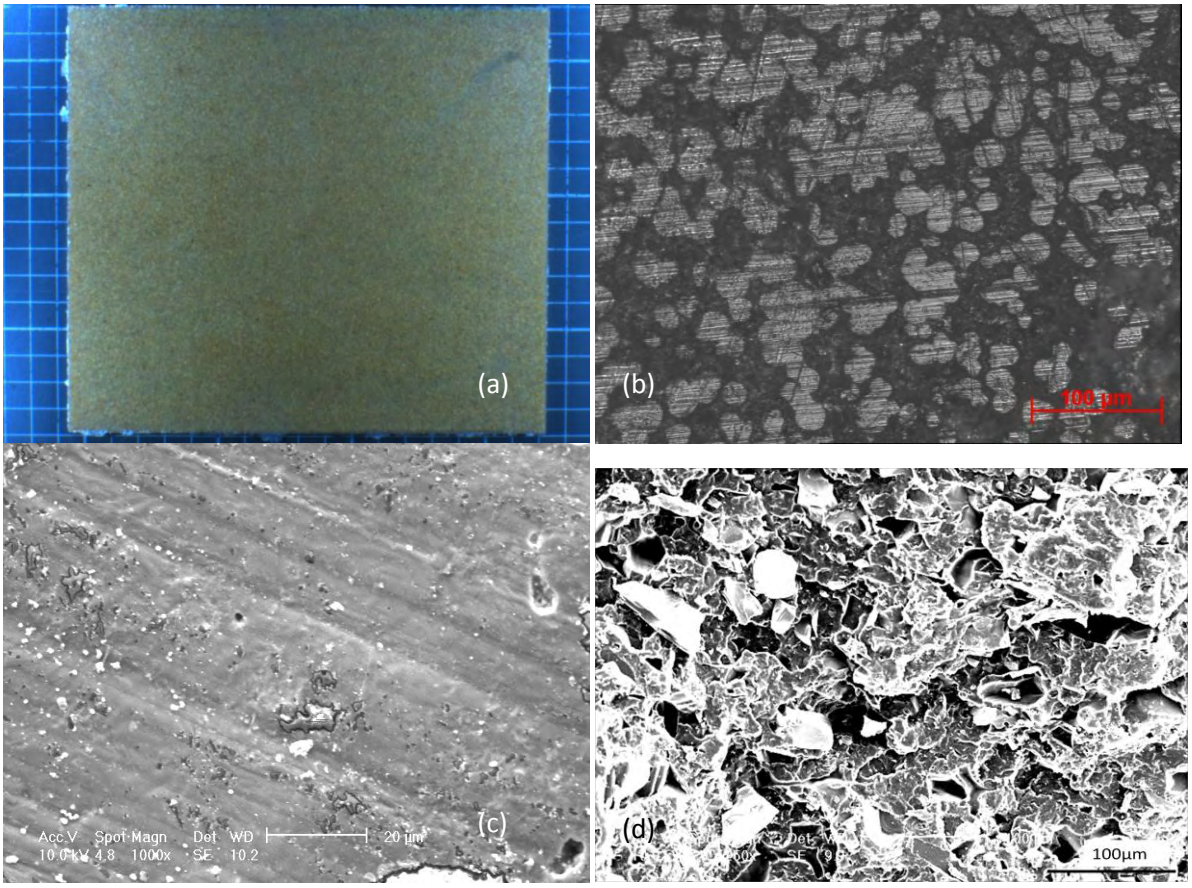

Figure 10 (a) Synthetic Ice sample plate, (b) Synthetic Ice surface image, optical microscopy, (c) Synthetic Ice surface, SEM, (d) Synthetic Ice cross section, SEM

3.6 Sliding Testing

Prior to the initiation of testing, profiles of untreated and treated blade samples were examined using a profile-meter. A comparative profile was established following the completion of the wear testing. Profiles were over-laid and a volumetric comparison was established to determine material loss during the wear testing. To obtain the profile a special holder was produced to ensure that all profiles were taken at the same edge angle. A 3-D profile for each blade was generated by repeatedly scanning the surface of the edge, for each profile, which is representative of an area of 3 mm of edge, 120 scans were required. To generate a profile, each scan recorded for a length of 1 mm, at a speed of 0.1 mm/sec, measuring to a surface finish of 100 µm.

Following completion of wear simulation testing and calculation of material volume loss through 3-D blade profiling, the wear factor was calculated using the principles of the Archard Equation, which is outlined in equation 3 [76-80].

Equation 3 - Archard's Equation

$$W = K \times s \times P$$

Where: W = volume loss K = coefficient of wear/wear factor

P = Applied Load s = sliding distance/wear

This can be rearranged to give an equation to calculate the wear factor;

$$K = \frac{W}{s \times P}$$

With the wear factor (K) being given in the units of cubic metres per Newton metre, m^3/Nm.

Blades were weighed pre and post testing in order for a weight loss comparison to be established, for each of the sample blades, to obtain a rough value for volume loss of the edge sample as a result of exposure to the wear testing.

Wear testing was carried out using a Tribometer TE70, reciprocating wear machine, figure 11. Untreated and treated blades were run against the synthetic ice samples, under a loading of 2000 g for 5000 cycles. The sliding distance for each cycle was fixed at 15 mm. In order to properly carry out the wear testing a specialised holder was produced in order to

attach the blade at the correct angle of incidence 25^{o} offset from vertical, against the synthetic ice. Each of the tests required an average of 14 hours to run to completion.

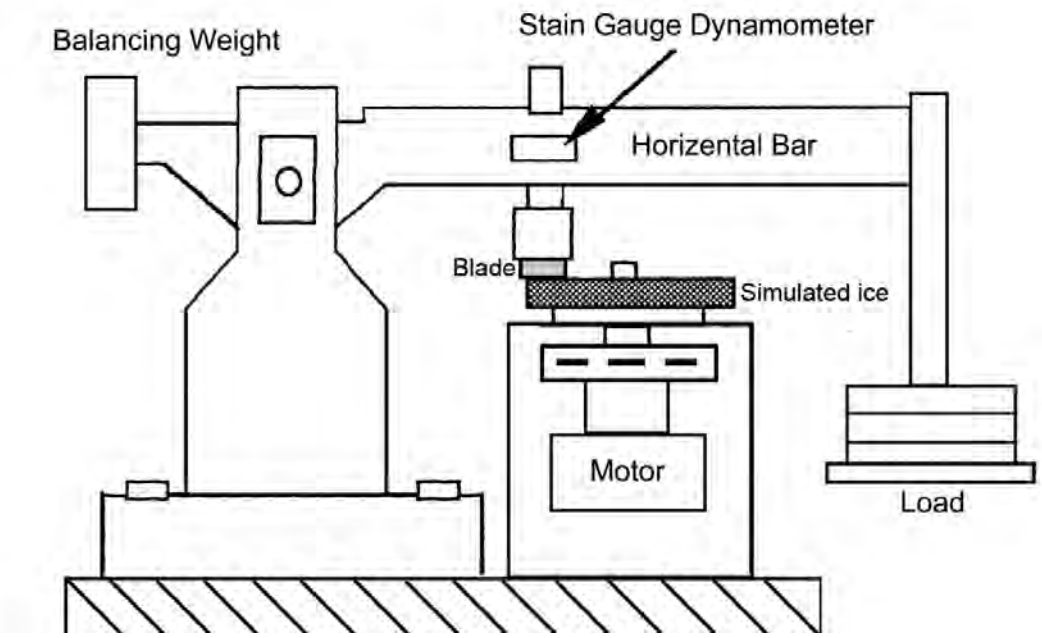

Figure 11 Set up for sliding simulation testing

4 Results

4.1 Sample Discs

4.1.1 Microstructure

Initial investigation on the microstructure of the modified layer was carried out using both optical microscopy and SEM, with a chemical analysis being carried out using EDX. Optical microscopy of plasma surface alloyed AISI 316 presents findings consistent with those seen in previous studies, whereby the modified S-Phase region can clearly be seen, as a smooth white region for the austenitic samples, as shown in figure 12. For the carburised samples, figure 12 (a) and (b). It can be seen that whilst both samples show a modified region which is smooth and “white” in appearance, there is a marked difference in layer thickness between the treatment at 450^{o}C and that at 500^{o}C, with the latter showing a greater depth of modified layer than the former. In a comparison of the nitride samples, figure 12 (c) and (d), a similar difference can be seen between the treatment carried out at 400^{o}C and that carried out at 450^{o}C. This is true also of the carbo-nitrided samples.

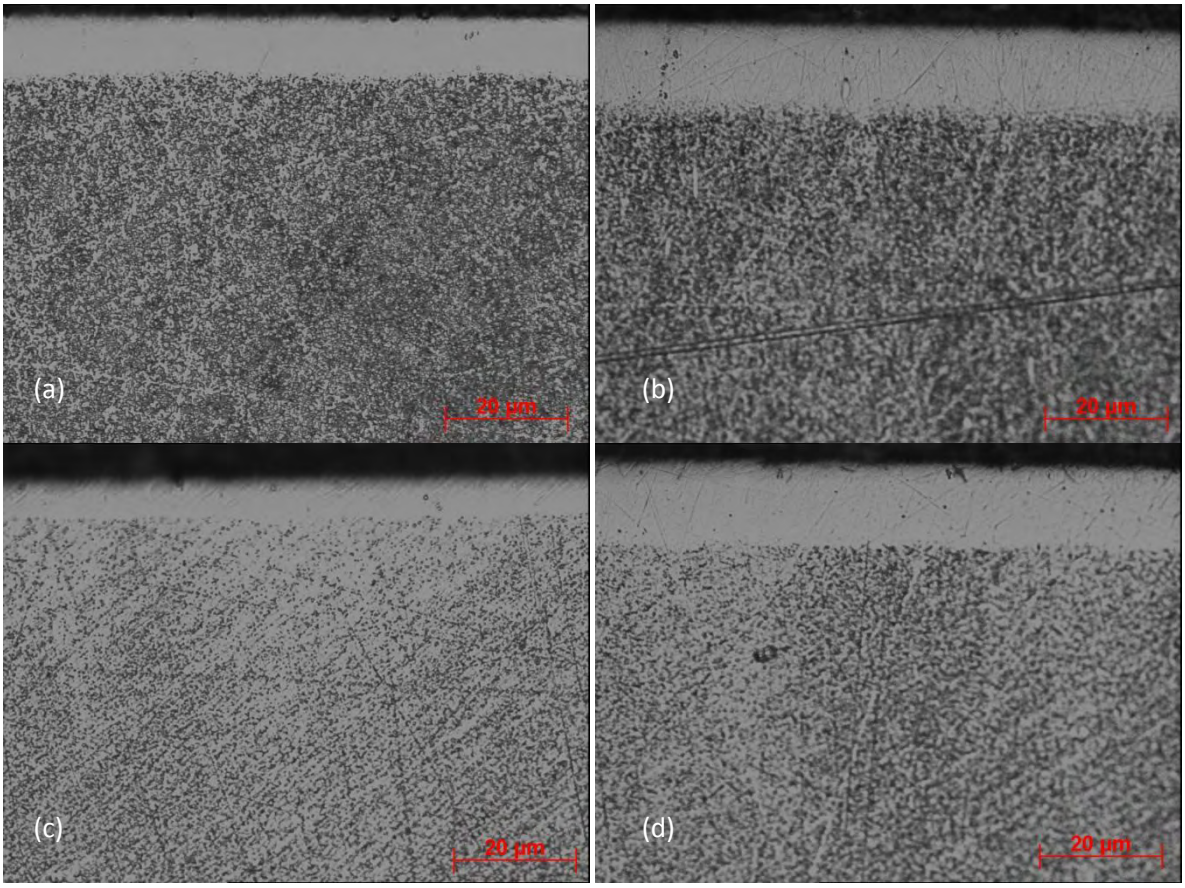

Figure 12 Austenitic Samples under optical microscopy, clockwise from top left: (a) carburised 450°C, (b) Carburised 500°C, (c) Nitrided 450°C, (d) Nitrided 400°C

During the course of the study it was also observed that the thickness and quality of the modified layer differed between the nitrided and carburised samples. Nitrided samples exhibited a much shallower depth of diffusion for the alloying element than the carburised samples. However, it was also observed that the nitrided samples exhibited a greater percentage of the alloying element present in the modified region than the carburised samples.

Figure 13 provides an example of SEM analysis of the austenitic samples, from the images it is possible to obtain a better impression of changes in the microstructure in the parent substrate when compared with the modified S-phase region. It is commonly accepted that

the S-phase shows a featureless microstructure as a bright layer. This layer, however, is metastable and precipitation may occur at higher temperature. It has been shown in figure 13, there are dark regions in the modified PN modified layer which are the precipitates formed during alloying treatments. These dark regions seen, in figure 13 in the modified layer represent typical formation of precipitates, it can be seen though that this is occurring on a very small scale.

Figure 14, shows a typical point scan for an EDX chemical profile in austenitic samples following carburising, with a slight elevation in the levels of carbon detected.

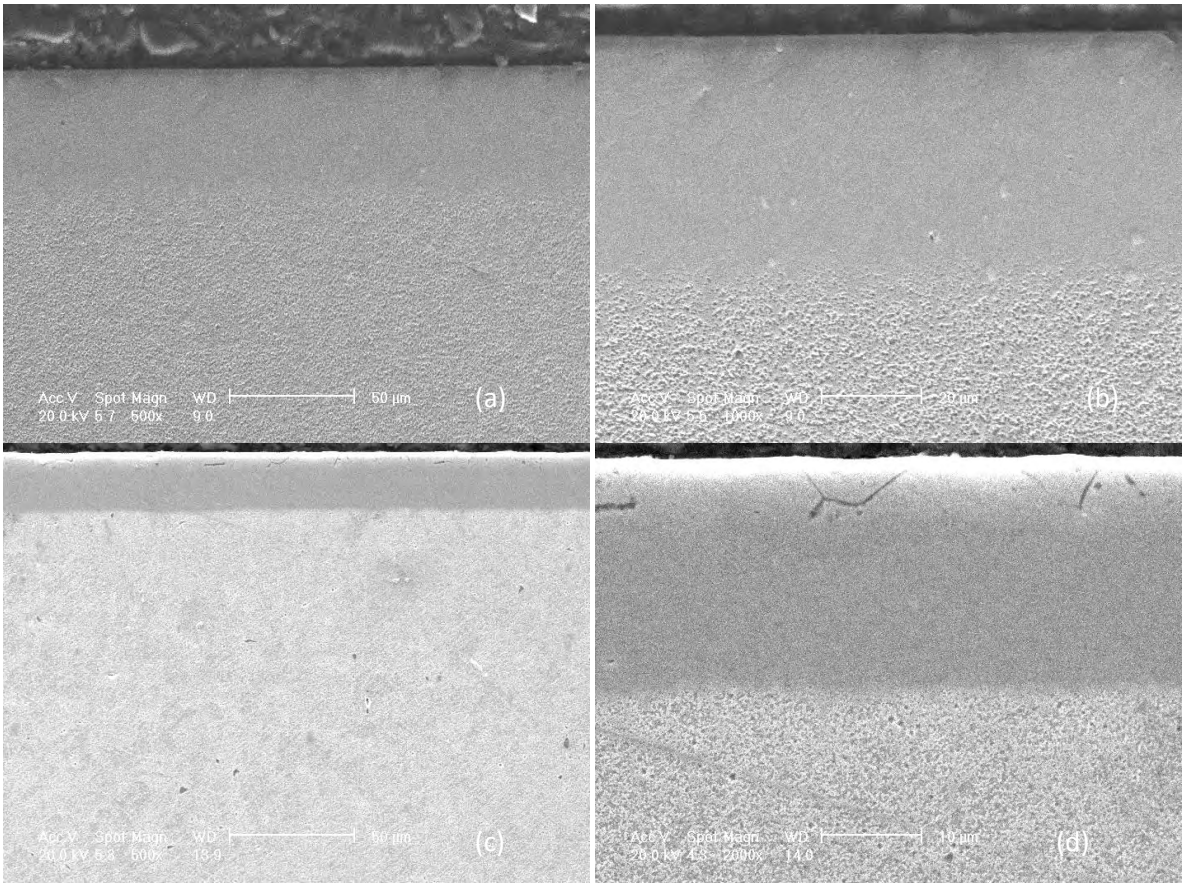

Figure 13 Austenitic sample disc's under SEM, clockwise from top left: (a,b) Carburised 500^{o}C, (c,d) Nitrided 450^{o}C

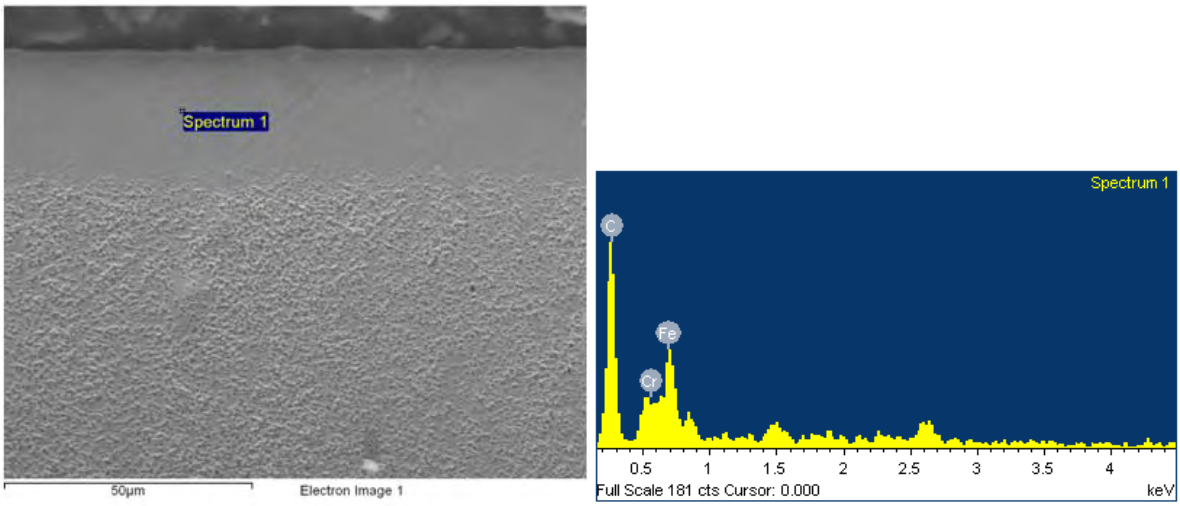

Figure 14 Austenitic carburised 500°C, EDX chemical analysis

In figure 15, martensitic samples examined under optical microscope provide initial information as to the effectiveness of the treatment process. Both the carburised and nitrided samples show an increase in diffusion depth of the modified layer with an increase in the treatment temperature. Several other observations can be made concerning the modifications, unlike the austenitic samples, there is not such a marked difference in the diffusion depth between the plasma carburising and the plasma nitriding treatments. It is also notable that the modified regions do not exhibit the same smooth appearance as the s-phase region seen in the austenitic samples. This is further exhibited in the optical micro-graphs, where the modified layer is seen not as a bright white region but rather as a lighter layer in the surface region. Previous research has indicated that this is owing to the fact that as opposed to being a typical S-phase layer as seen in austenitic samples, the modified region takes the form of a compound layer over a diffusion zone. This lighter region is typical of a diffusion zone evidencing the formation of precipitates, which it has been suggested may be chromium nitrides or carbides respectively depending on the treatment.

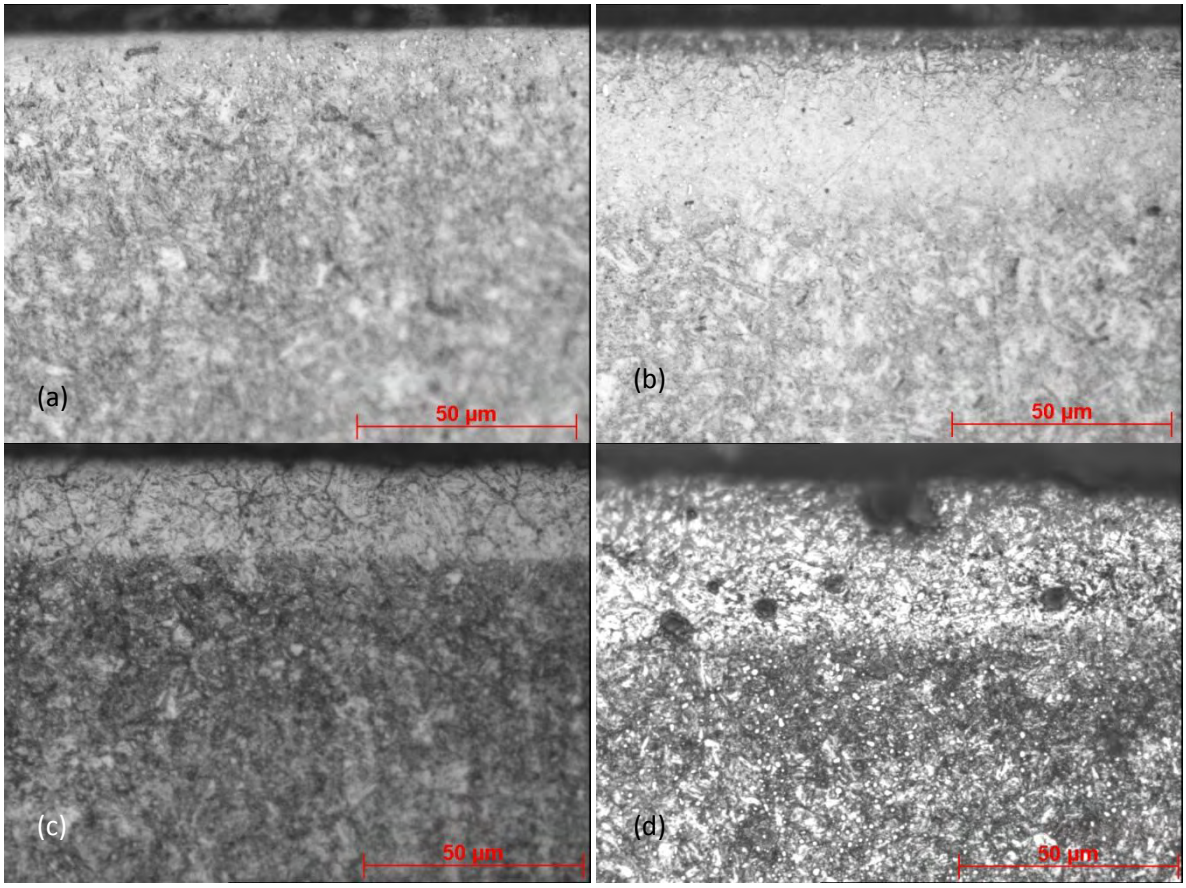

Figure 15 Martensitic sample disc's under optical microscopy, clockwise from top left: (a) Carburised 450°C, (b) Carburised 500°C, (c) Nitrided 500°C, (d) Nitrided 450°C

Further to this examination high magnification analysis has been carried out using SEM. Results from the SEM analysis can be seen in figure 16. Indication from data obtained suggests that the modified region is indeed a compound layer, with the presence of precipitates being found therein. This is especially evident in the nitrided samples, in figure 16 (c,d). Where the modified region exhibits a different microstructure to that seen in the bulk material. It is also evident in these micro-graphs that the samples have been exposed to severe corrosive attack; this is due to the etching process used during this study. This attack during etching can be traced back to the modified region being rich in precipitates, probably Cr_xN_y, which results in some depletion of the natural corrosion resistant properties of stainless steels.

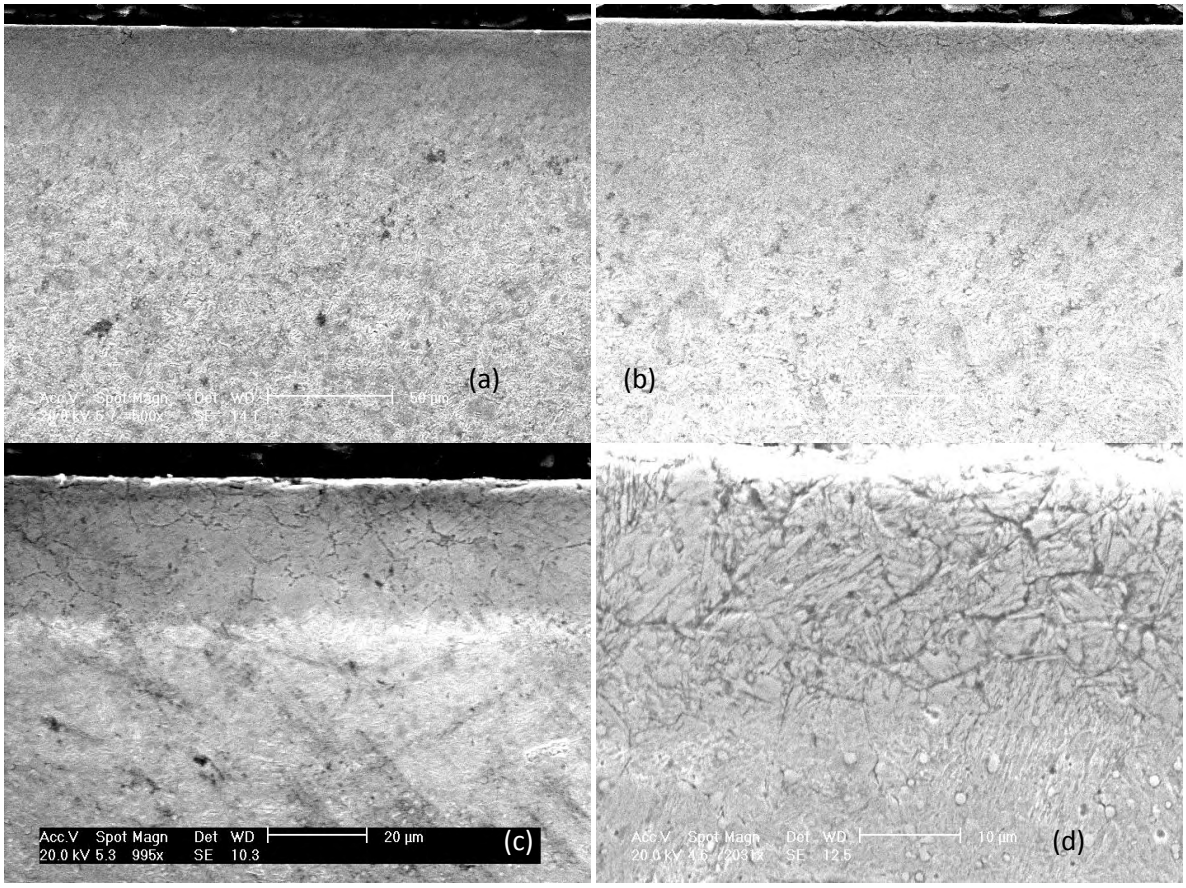

Figure 16 Martensitic sample disc's under SEM, clockwise from top left: (a,b) Carburised 500°C, (c.d) nitrided 450°C

Furthermore EDX analysis of the modified layer, figure 17 has revealed that the chromium content in the modified layer has been reduced significantly from that seen in the bulk material, in the carburised samples, from 17 % by weight down to 13 % (±1 %). Whilst in the nitride samples the chromium content has remained similar in the modified layer when compared to the bulk substrate, in the region of 13 % (±1.5 %) by weight. In addition to this EDX has revealed that in the carburised samples there has been an increase in the carbon content found in the modified layer, it is difficult to obtain an accurate carbon content using EDX analysis. In the nitrided samples a corresponding increase in the nitrogen content in the modified layer is seen, with an increase to a maximum of 4.7 % ±(0.5 %). For carburised samples there has been very little change in the Iron content by weight, with the expansion in the parent lattice being compensated for by a reduction in chromium content. However,

for nitride samples there has been a significant drop in the iron content in the modified region, which can be associated with an increase in the nitrogen content.

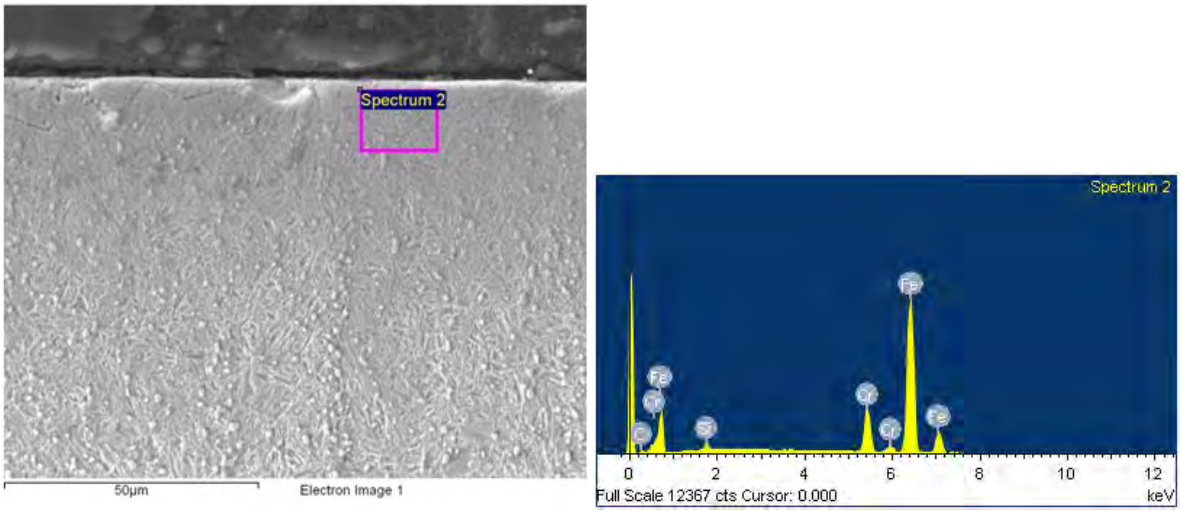

Figure 17 Martensite carburised 500°C, EDX chemical analysis

Carbo-nitriding treatments in martensitic samples yielded similar results to those seen, in the nitrided and carburised samples. A shallow compound layer is observed in the diffusion zone in the immediate surface region, combined with a deeper diffused layer which exhibits the smoother structure more similar to that seen in the s-phase region in austenitic samples. The shallow compound layer is produced following nitriding treatment, whilst the deeper modified layer is achieved following the carburising treatment.

4.1.2 Chemical Analysis

Following GDOES examination of the surface treated layer of the disc samples, the chemical composition depth profiles were obtained for the alloyed nitrogen and carbon of the treated samples. Diffusion depth profiles for the nitrided austenitic (AISI 316) and martensitic (AISI420) samples can be seen in figure 18(a) and (b) respectively. Figure 19 (a),

shows the diffusion depth profile for the carburised austenitic (AISI 316) and martensitic (AISI 420), figure 19 (b), disc samples at each of the chosen temperatures respectively.

It can be seen in both the martensitic and the austenitic samples that as the treatment temperature is increased, then the depth to which the nitrogen and carbon ions diffuse increases accordingly.

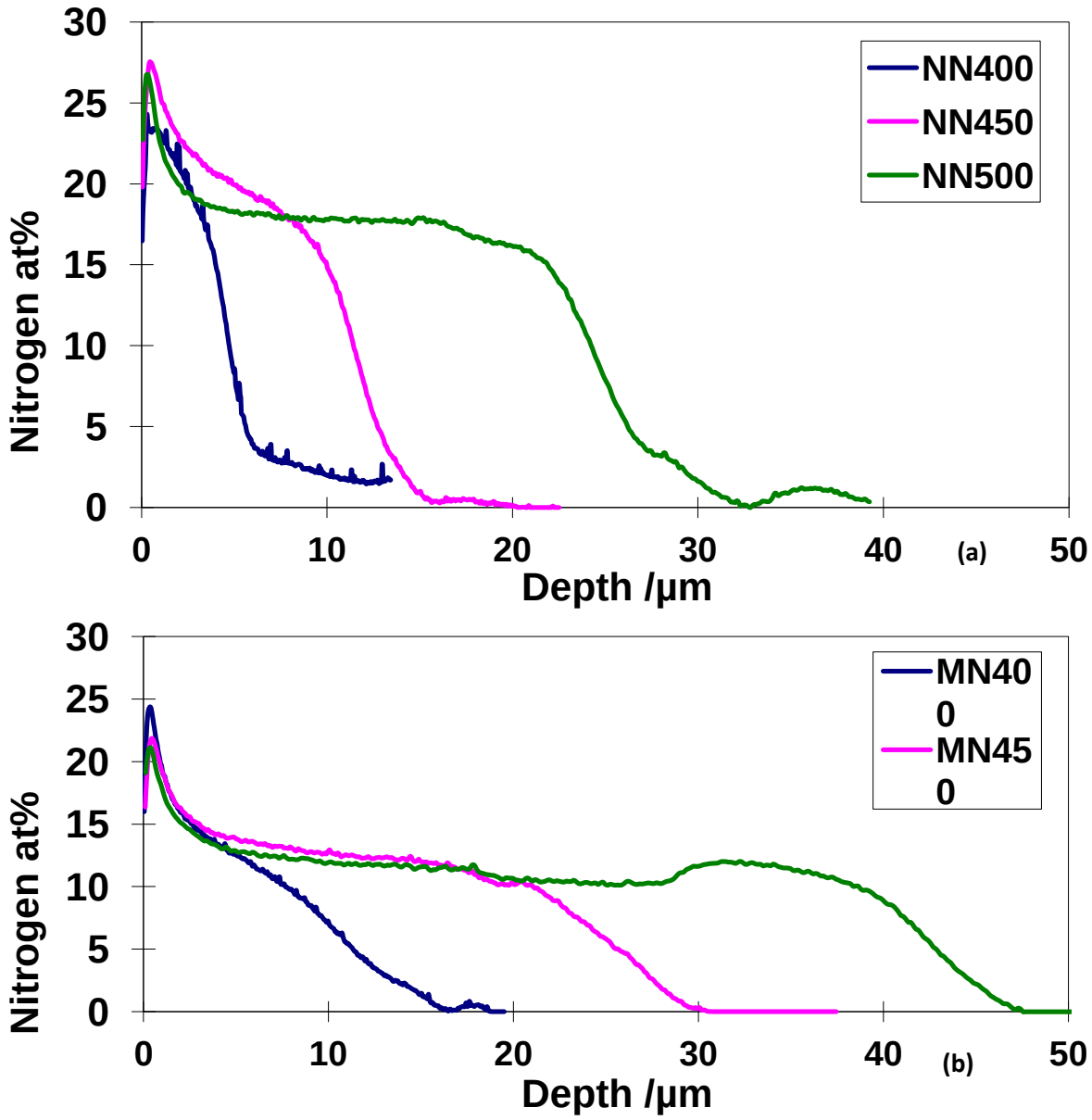

Figure 18 Nitrogen GDS diffusion profiles for (a) AISI 316, (b) AISI 420

In the austenitic samples results indicate, that carburising generates a greater diffusion depth than that seem in the nitriding samples. Nitrided samples produce a diffusion depth less than 12 µm for temperatures of 400^{o}C and 450^{o}C, and in the region of 20 µm for 500^{o}C treatment. Compared with the carburised samples producing diffusion depths greater than 20 µm for both the 450^{o}C and 500^{o}C, and in the region of 15µm for the 400^{o}C treatment. However, nitriding produces a greater percentage change in surface chemical composition, when compared with that seen in the carburised samples. What can also be seen is that diffusion profile of nitrogen exhibits a much sharper drop from the elevated level back to base composition, than that exhibited by the carburised samples.

Results from the martensitic samples indicate a similar trend to those shown in the austenitic samples, with an increase in diffusion depth linked to an increase in the treatment temperature. Results also indicate that nitriding produces a greater percentage increase than that seen in the carburised samples, in the surface region. However, with regards to the diffusion depth shown, there are certain differences to that seen in the austenitic samples; indication is that, the carburising treatment has not been as effective for the martensitic samples. This is seen in a sharper diffusion gradient, owing to the shallower depth of effective treatment, than that seen in the austenitic samples. As with the austenitic samples once a case depth of 10 µm has been reached in the nitride layer then a rapid drop in the nitrogen composition is seen.

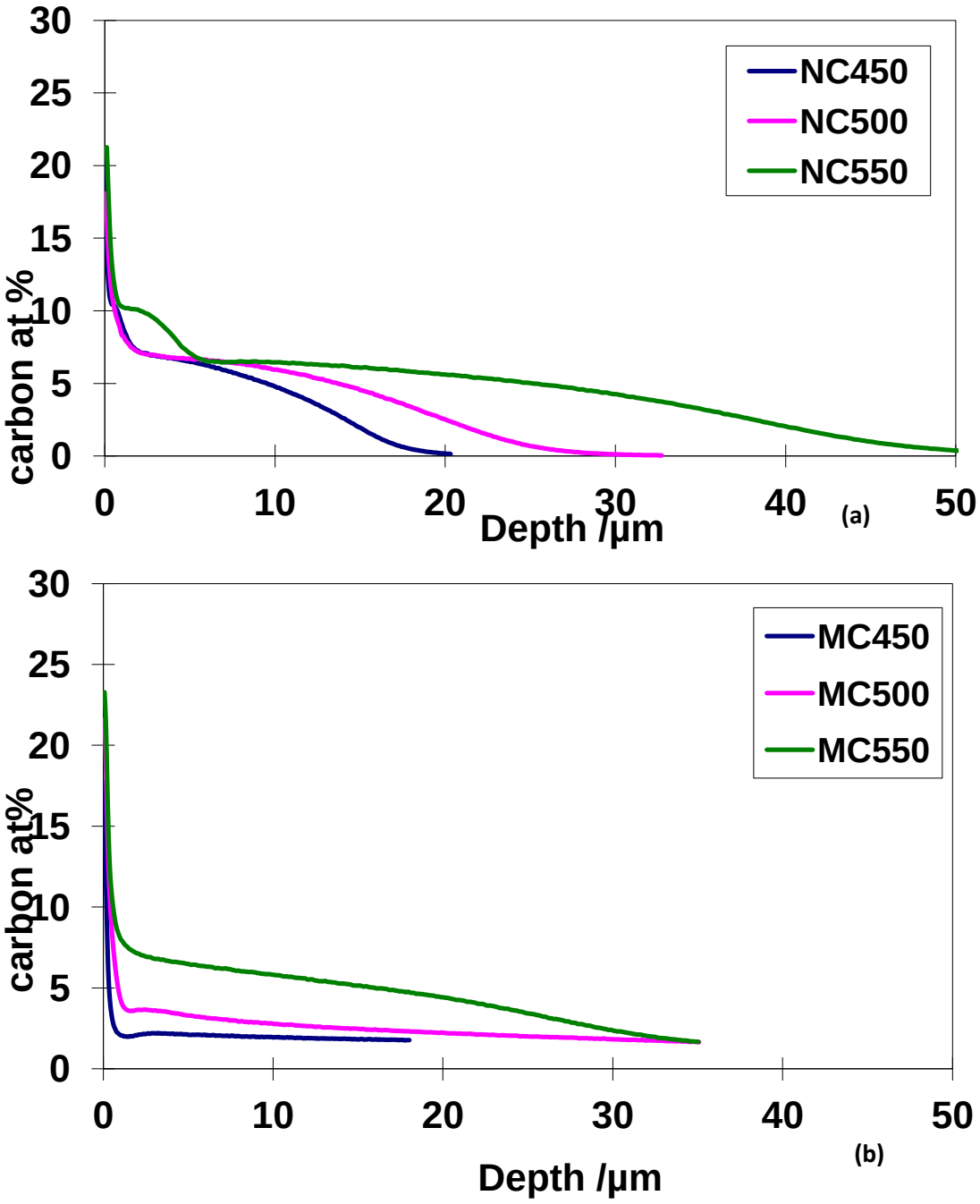

Figure 19 Carbon Diffusion depth profiles for (a) AISI316, (b) AISI420

Further to the results obtained from the nitriding and carburising, GDOES was also carried out on the carbo-nitrided samples in order to compare the diffusion depth of carbon and nitrogen during treatment in a combined atmosphere.

4.1.3 Surface Hardness

Surface hardness results for disc samples are shown in figure 20. It can be seen that all the treatments have resulted in an improvement when compared with the surface hardness of the parent substrate material. Inherently martensite is harder than austenite, due to the quenching, the result of which is that a smaller percentage improvement in surface hardness is seen.

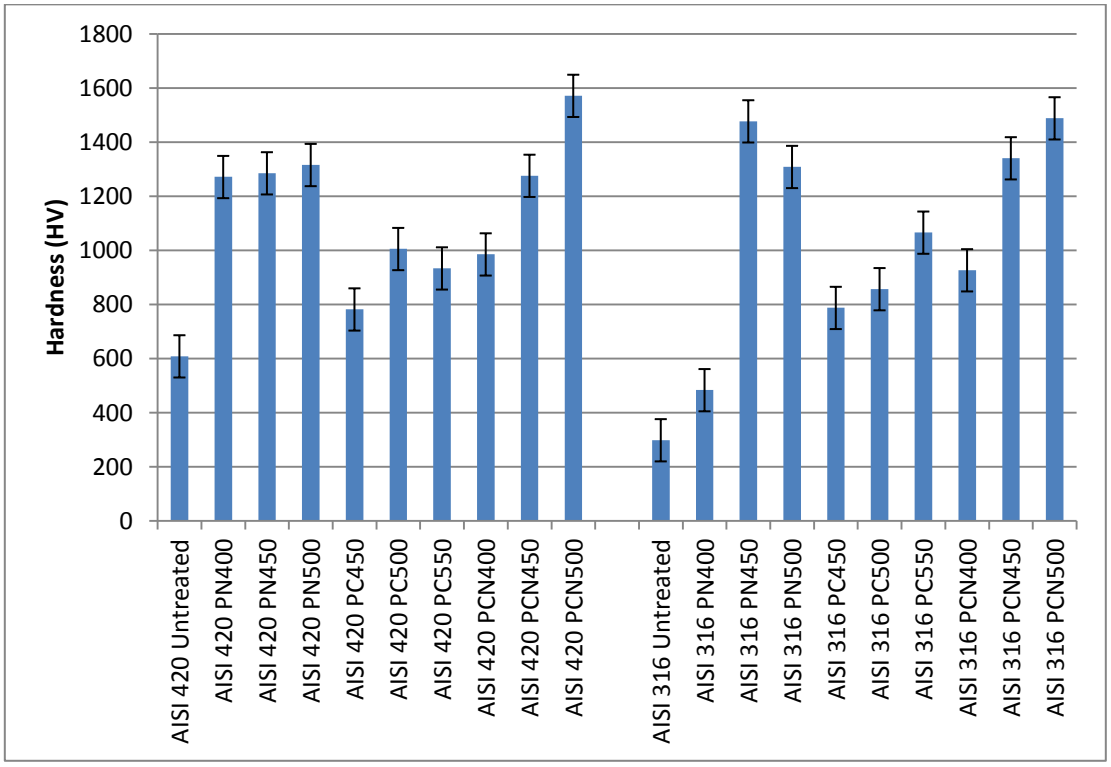

Figure 20 Surface Micro-Hardness of AISI316 and AISI420 sample discs

From the results obtained it has been possible to ascertain the following information; (1) all forms of modification have resulted in a great increase in the surface hardness of the bulk material, (2) for both martensitic and austenitic samples, nitriding has produced a greater improvement in surface hardness than that seen as a result of carburising, (3) there is a corresponding improvement in surface hardness related to an improvement in the specific treatment temperature. There is one exception to this rule in the results obtained; this is

seen in the AISI 420 sample carburised at 550^{o}C, where there is a drop in surface hardness when compared with the lower temperature of 500^{o}C.

In carbo-nitrided samples there is a greater effect of treatment temperature on the resulting improvements to surface hardness. This is evident when increasing the treatment temperature above 400^{o}C, where an improvement of roughly 150 % over the original parent substrate hardness is seen, for both the austenitic and the martensitic samples tested. This sudden improvement is likely owed to the combined hardening effects of both nitriding and carburising, coupled with an increase in temperature which is known to improve diffusion depth.

4.1.4 Cross Sectional Micro-Hardness

The hardness measured using a Knoop indenter along the cross-section of the surface layer is shown in figure 21, figure 22, figure 23. For the treated AISI 316 samples figure 21 (a), figure 22 (a) and figure 23(a), it has been determined, that all of the modifcations have had an influence on the hardness of the near surface region. For the nitrided samples figure 21 (b) figure 22 (b) and figure 23 (b) it can be seen that there is a sharp drop in the hardness profile with a large reduction in hardness from the levels seen in the surface region, once a depth of 8µm has been reached. This sharp profile drop results in a return to the intrinsic hardness of the parent material, by a depth of 12µm form the surface. In the carburised samples the hardness profiles exhibited was much shallower, than that seen for nitriding, indicating that it is a much more constant and gradual decline in hardness through from the surface into the bulk material. Carburised samples also exhibit a deeper effective depth of diffusion, in the case of the 500^{o}C treatment seen in figure 21, the depth is measured at 25µm. Generally it would be expected that the carbo-nitrided samples would exhibit a

profile somewhere inbetween that shown by nitriding and carburising, however in the case of the AISI316 450^{o}C sample, the profile seen is more similar to those traditionally seen in nitrided samples.

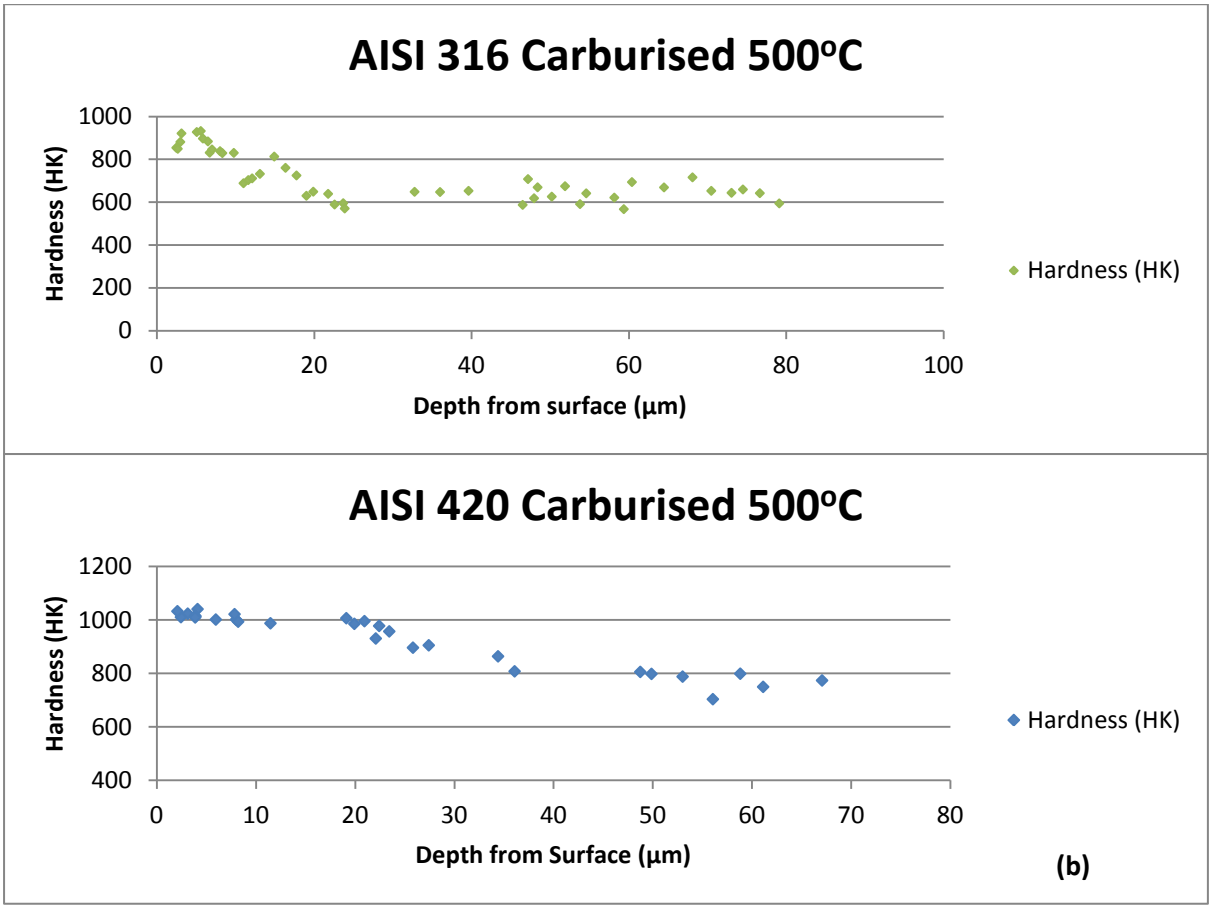

Figure 21 Cross-sectional hardness of carburised disc samples (a) AISI316, (b) AISI420

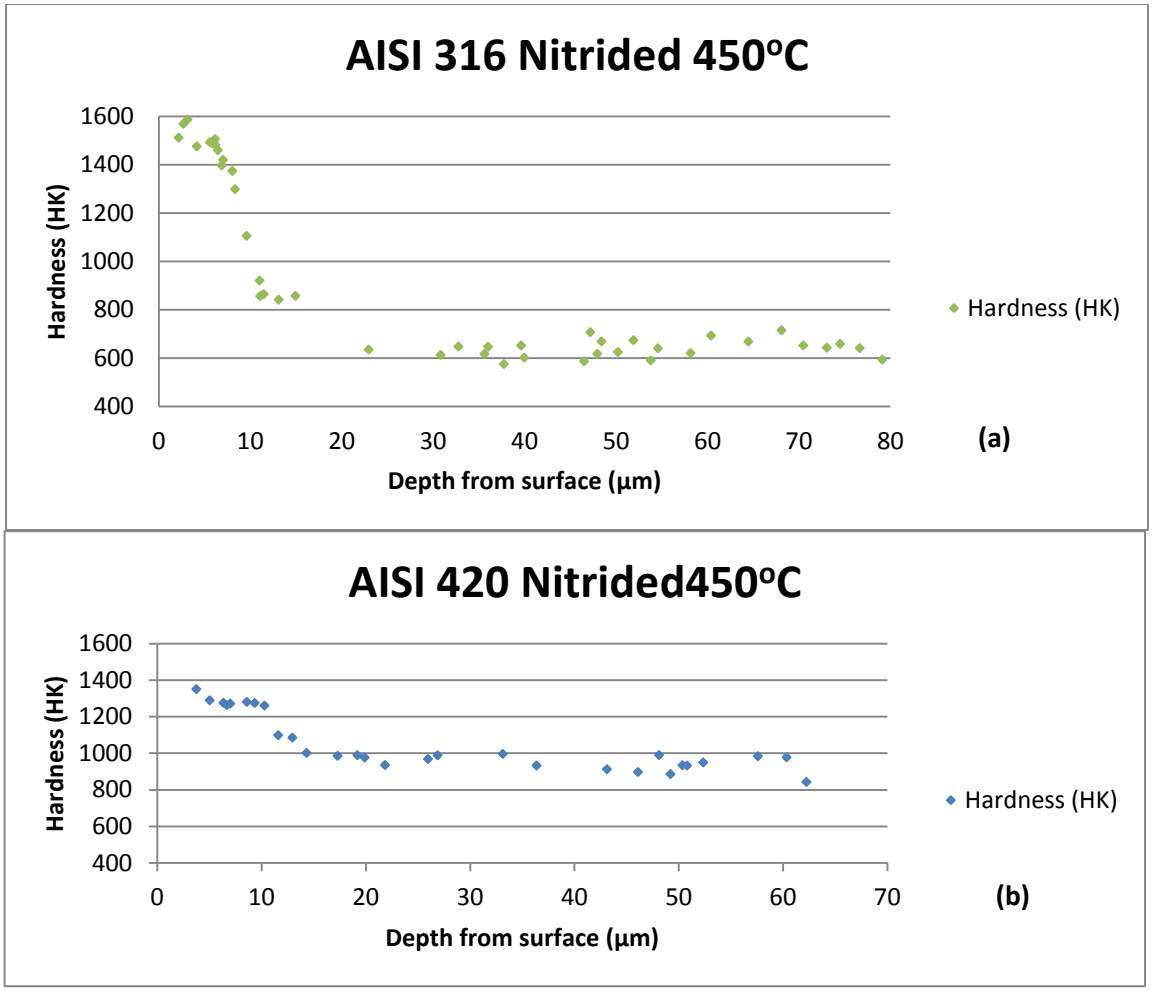

Figure 22 Cross-sectional hardness of nitrided disc samples (a) AISI316, (b) AISI420

When considering the martensitic samples, the hardness depth profiles revealed the following; in the case of nitriding, profiles are similar to those seen in the nitride austenitic samples. In the case of the 450^{o}C sample the effective diffusion depth is in the region of 10 µm, at this depth there is a sharp drop in hardness, back to that show by the parent bulk material. In both the carburised and carbo-nitrided samples, profiles are similar, with a shallow profile exhibited, and a consistent smooth drop in hardness, through the modified region into the bulk parent material.

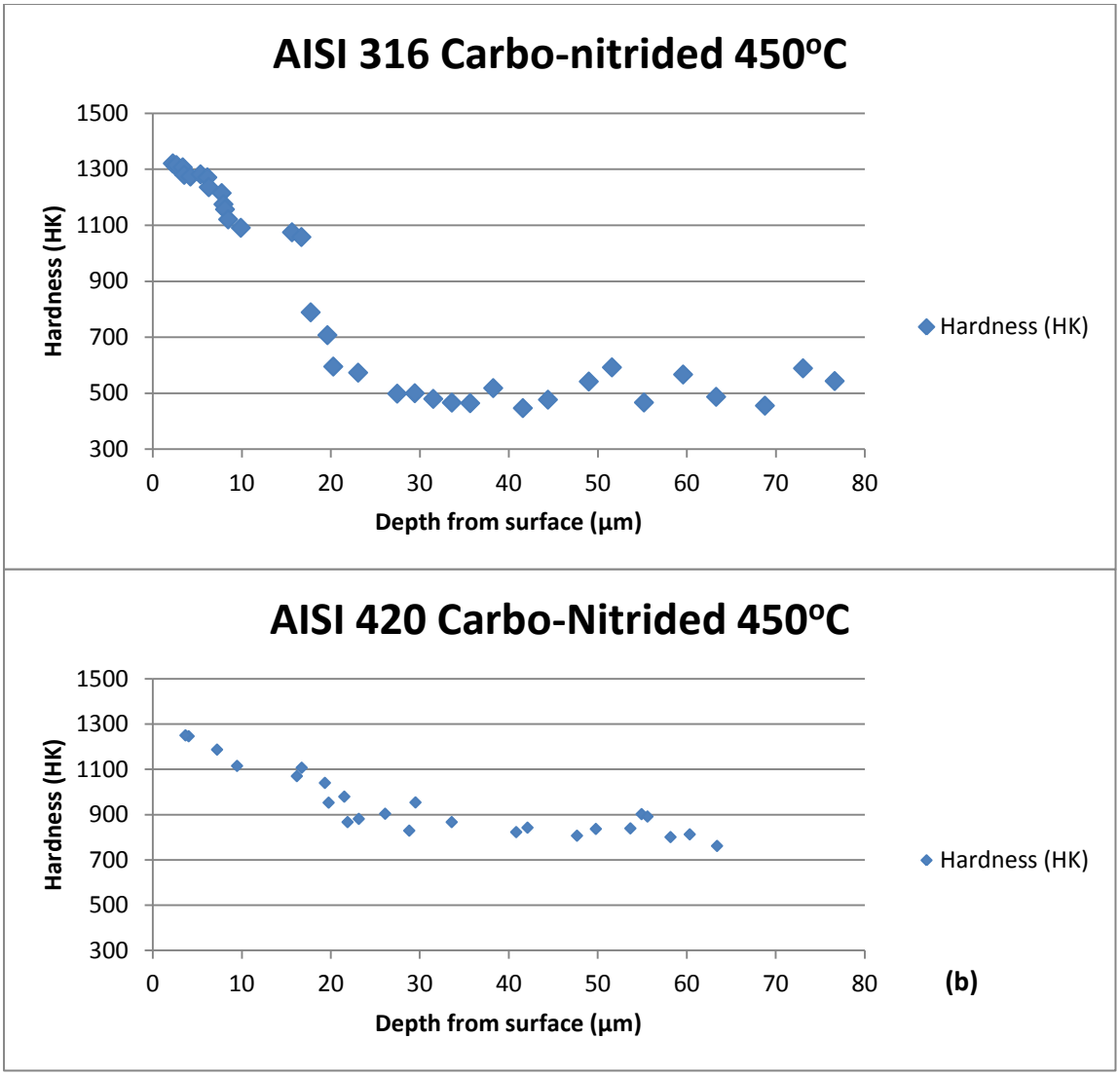

Figure 23 Cross-section hardness of Carbo-Nitrided disc samples (a) AISI 316, (b) AISI420

4.1.5 Corrosion

The weight loss of the samples was recorded at 72 hours and at 192 hours. Based on the weight loss measurements the rate of corrosion was calculated in; µm/year.

Table 6 Disc sample corrosion rate following 72 and 192 hours immersion in 3.5%NaCl

Sample	Corrosion rate 72 hours (μm/year)	Corrosion rate 192 hours (μm/year)
AISI 316 Untreated	249.32	124.5
AISI 316 PN450	317.53	154.70
AISI 316 PC500	245.97	111.9
AISI 316 PCN450	391.32	165.6
AISI 420 Untreated	658.44	293.7
AISI 420 PN450	624.38	276.75
AISI 420 PC500	442.75	212.9
AISI 420 PCN450	544.92	259.7

From the extrapolation of corrosion rate for an annual rate, table 6 and figure 24, several observations have been determined. Initially it can be seen that as expected the untreated austenite is considerably more resistant to corrosion than the martensitic samples. It can further be seen that whilst in the austenitic samples the various treatment forms have had a marginal effect on the corrosive properties of the parent substrate, in the martensitic samples there has been a marked improvement in the corrosion resistance in all of the samples.

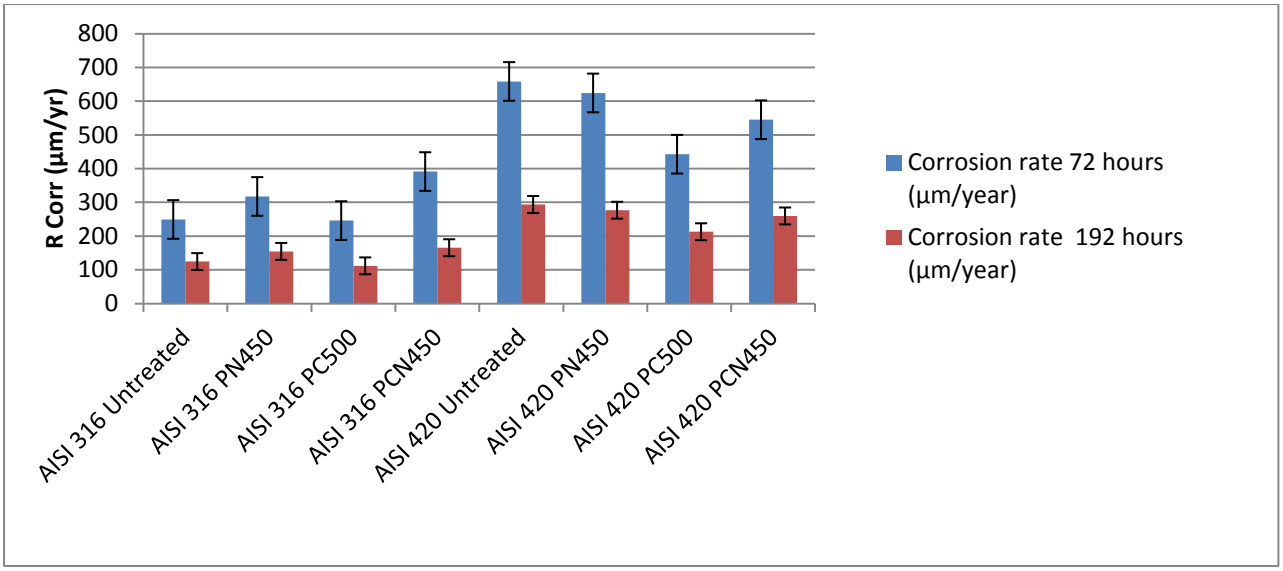

Figure 24 Corrosion rate of sample discs following 72 and 192hours immersion in 3.5%NaCl solution

It can be seen that for both austenitic and martensitic disc samples carburising has had the greatest positive effect on the resistance of the specimen to corrosion in 3.5 % NaCl, with carbo-nitriding having the next greatest impact. Furthermore it has been possible to determine that, as the period of time for which the samples are exposed to the corrosive environment is increased, then the more the rate of corrosion is slowed. This is seen for both the austenitic and martensitic specimens, in both the untreated and the modified samples respectively.

As can be seen from figure 25 (a,b), untreated sample surfaces exhibit typical examples of pitting corrosion sites in stainless steels [65, 81, 82]. Pit sites, are surrounded by a deposit of corrosion product, which is likely FeOOH, or rust, further examination is required to determine exact composition. Those pits which have experienced the most severe exposure to corrosive attack can be seen to be larger in size, and are likely sites which have formed as stable dominant pit sites.

Figure 25, shows SEM characterisation of sample disc surfaces following immersion in 3.5 % NaCl for a period of 192 hours. It can be seen that both the nitriding and carburising modifications have produced a reduction in the number of initiation sites for pitting corrosion; this indicates that the amount or corrosion has been reduced. This agrees with the calculated results obtained for corrosion rate. It can also be seen that the carburised samples have shown even greater resistance than the nitrided samples with an even smaller number of initiation sites visible.

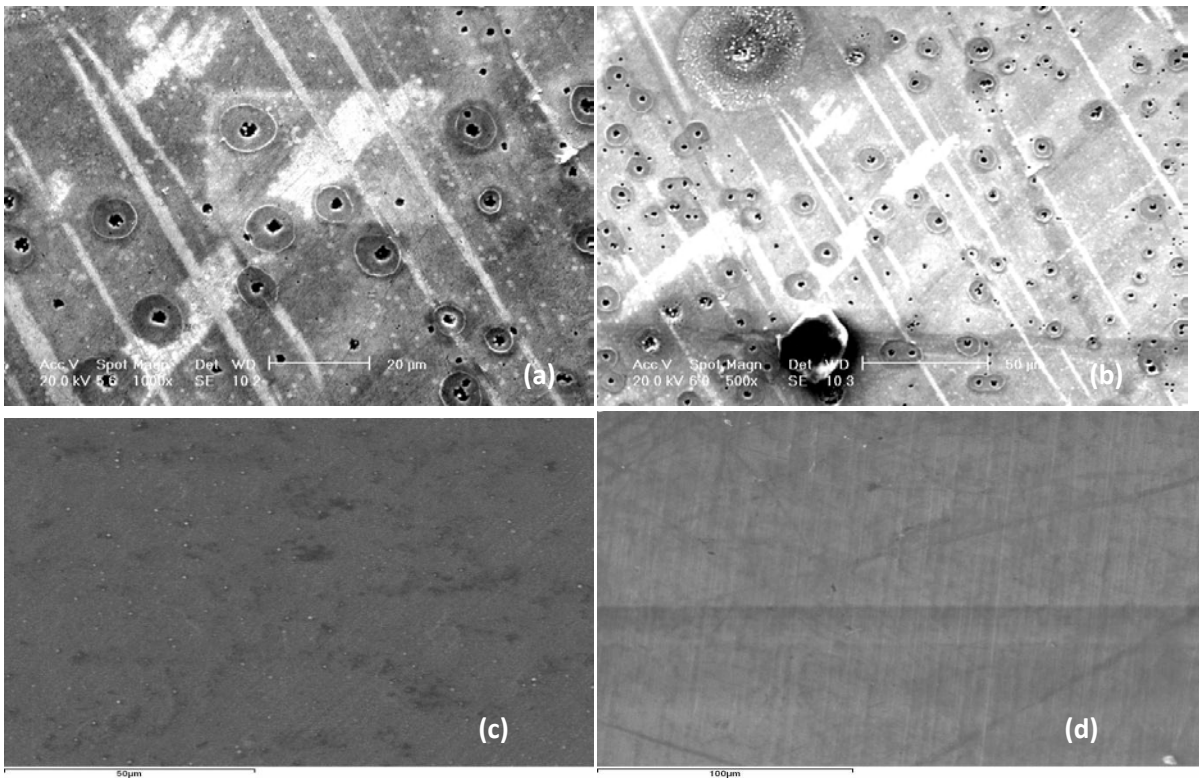

Figure 25 (a,b) Untreated AISI420 disc sample surface following 192 hours immersion in 3.5 % NaCl, exhibiting examples of formation of pitting corrosion sites, (c) Nitrided AISI420 disc sample surface, (d) Carburised AISI420 disc sample surface; following immersion in 3.5 % NaCl solution.

4.1.6 Summary of Disc Results

In summary the results obtained indicate that the plasma surface alloying treatments by nitriding and carburising methods to improve mechanical properties of the parent substrate without sacrificing corrosion resistance. Thus, as a result of these modifications conditions were selected to run simulation tests on a real ice skate blade, to obtain a combination of measurements to determine improvements in mechanical and wear properties. Selected treatment conditions for these simulation tests are carburisng and nitriding carried out at 450^{o}C for both AISI 316 and AISI420 samples.

4.2 Dummy Blades

4.2.1 GDOES

Glow discharge analysis of the dummy blades following treatment, revealed that as with the sample disc's modification has been effective at altering the chemical composition of the surface and near surface region of the specimen. Chemical depth profiles for the sample blades can be seen in figure 26. Similar results are observed to those observed for the dummy disc sample GDOES tests.

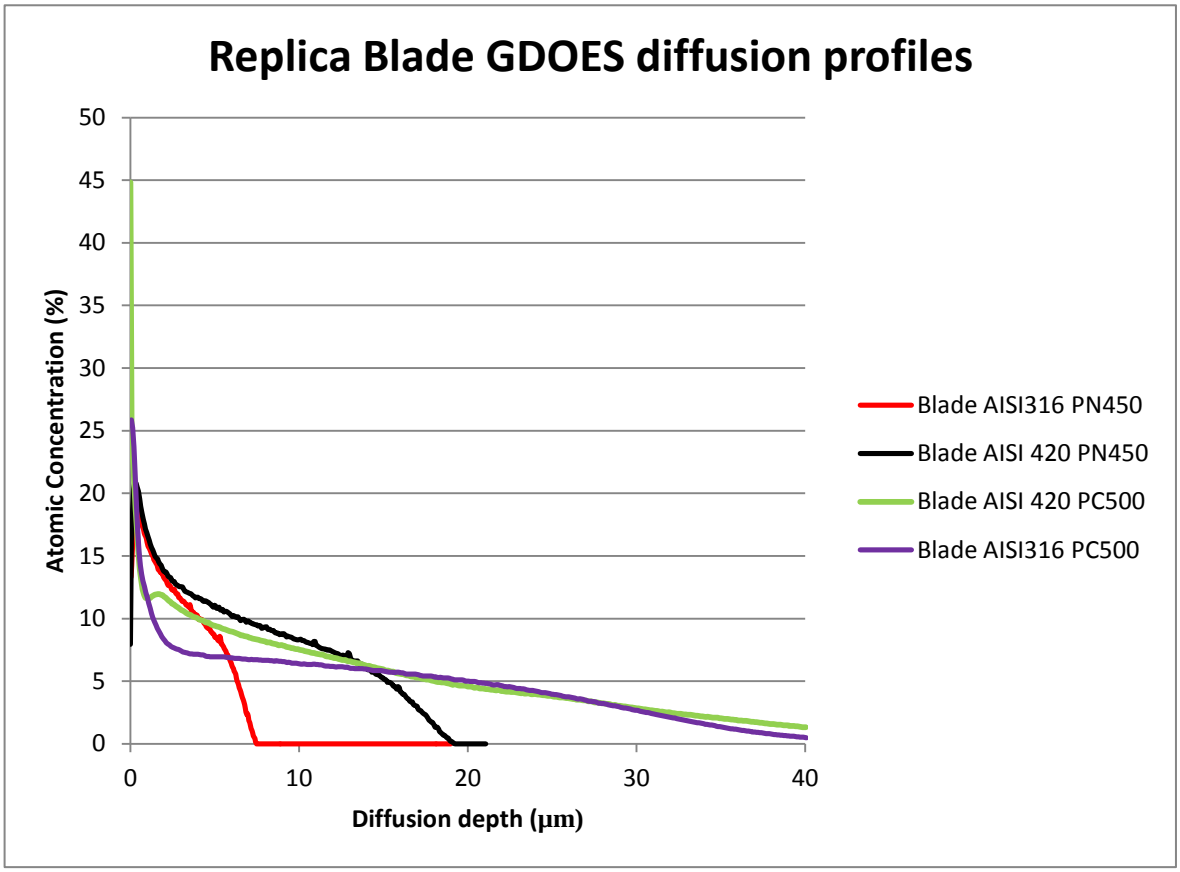

Figure 26 GDOES chemical diffusion depth profiles of replica blades following surface modification treatments

It has been determined that as with the sample discs, carburising, produces a greater overall diffusion depth of modification into the near surface region. For the nitrided blades it can be seen that similar profiles are observed for both the austenitic and martensitic samples, with a surface nitrogen content, in the region of 20 %, and an initial drop in nitrogen content at 3-4 µm, and a return to 0 % and pure parent substrate bulk material at a depth of 8µm for the austenitic blades, and 17 µm for the martensitic blades. Carburising has produced an almost identical profile for both the austenite and the martensite with a rapid drop occuring within 3 µm of the surface, from 25 % carbon, down to 8 %. Following this initial drop, a return to the parent substrate composition is more prolonged than that seen in the nitriding treatment with a depth of 35 µm being achieved.

4.2.2 Surface Hardness

Surface hardness, $Hv_{0.1}$ data was obtained for both blade body and edges for untreated and treated samples. From data obtained from surface hardness testing of the untreated and treated blades, it is possible to see that following treatment a marked improvement in hardness can be seen in figure 27. As with the sample disc's the greatest improvement in hardness is seen in the nitrided samples. Austenitic samples have shown the greatest percentage improvement in both nitriding and carburising treatments. This is owing to the naturally lower surface hardness of austenitic steels compared to that exhibited by martensitic samples.

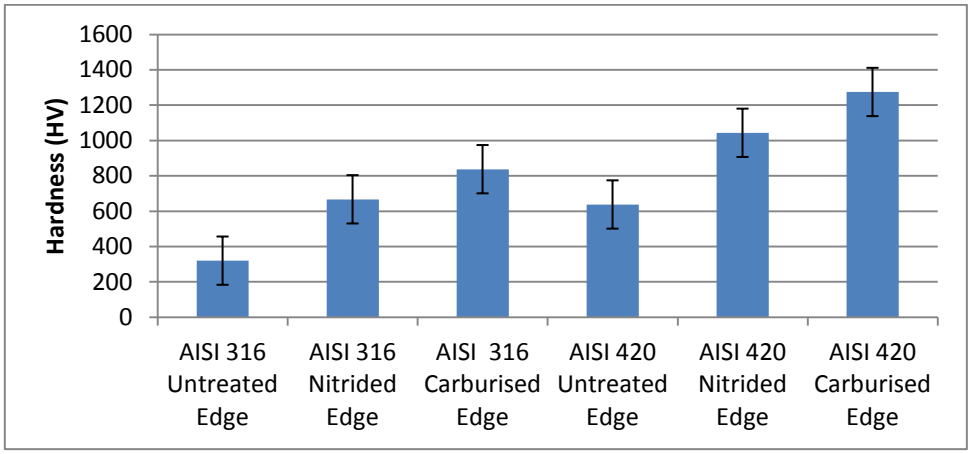

Figure 27 Surface Hardness measurements of replica blade edges, for untreated and modified samples

4.2.3 Wear

Prior to commencing sliding testing, edge profiles were obtained for each of the blade samples. Following sliding testing, a volumetric comparison was established between the wear loss experienced by the untreated samples, and that experienced by the treated

samples. A breakdown of the volumetric losses can be seen in table 7 along with the calculated wear factor. Wear factor results can also be seen in figure 28.

Table 7 Volume Loss and Wear Factor's for blade edge post wear simulation testing

Sample	Volume Loss (m^3)	Wear Factor (m^3/Nm)
AISI 316	$7.867x10^{-10}$	$2.674x10^{-13}$
AISI 316 PN450	$1.63x10^{-10}$	$5.541x10^{-14}$
AISI 316 PC500	$1.885x10^{-10}$	$6.407x10^{-14}$
AISI 420	$2.727x10^{-10}$	$9.269x10^{-14}$
AISI 420 PN450	$6.993x10^{-11}$	$2.377x10^{-14}$
AISI 420 PC500	$1.773x10^{-10}$	$6.027x10^{-14}$

When considering the volume loss seen in the specimens, following exposure to wear testing, it has been possible to determine the following; treated samples all show a considerable reduction volume loss of material when compared to the figures obtained for the untreated samples. It is important to note the data obtained for the untreated austenitic and martensitic samples, with martensitic samples exhibiting a smaller volumetric material loss than that seen in the austenitic samples. It is likely that this is due to the naturally higher hardness properties exhibited by martensite, which can be seen in both materials data for the two materials, and in the surface hardness testing results in sections for disc samples and replica blades respectively.

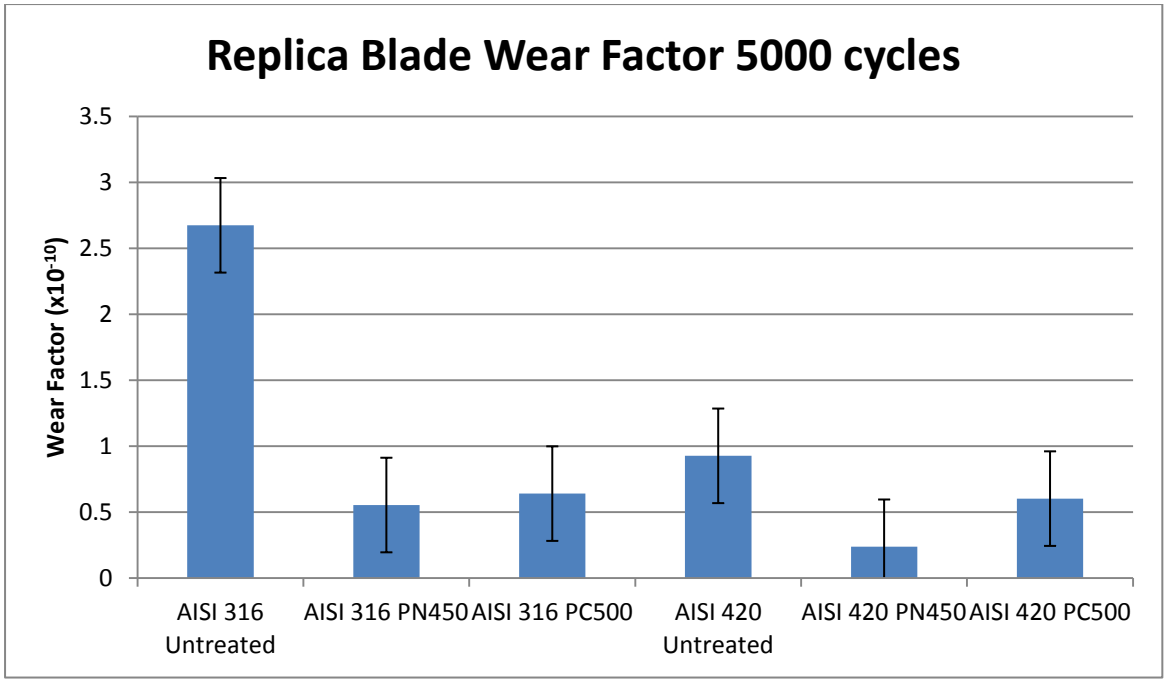

Figure 28 Wear factor through 5000 cycles of reciprocating sliding wear simulation

It can be seen for the austenitic samples (AISI316) that whilst both nitriding and carburising have reduced the volume loss of material during the simulation testing, comparatively nitriding has shown the greatest reduction in volume loss.

Following calculation of volume loss, the next step taken was to calculate the wear rate which the samples experienced. This was done using equation 3 based on Archard's principle[76], and the wear rate has been extrapolated to generate a figure for an annual rate of wear experienced by the replica blade samples during simulation testing. Results of the wear rate determination can be seen in table 7 and figure 28 wear factor through 5000 cycles of reciprocating sliding wear simulation.

A calculation of the wear factor for each of the replica blade specimens, has been calculated based on the results obtained from the volume loss, using equation 2. From the data in table 7 it can be seen that the wear factor which have been obtained for the untreated

samples, correspond to the results obtained from the volumetric material loss, whereby the austenite has undergone a greater amount of wear when compared to the martensite. Again this is to be expected and is likely linked to the intrinsically higher surface hardness seen in the martensite.

To further compare results, percentage improvements were calculated with the following information being obtained; for wear resistance improvements: AISI316 nitrided, 79 %, AISI316 carburised, 76 %, AISI420 nitrided, 74.6 % and AISI420 carburised, 34.9 %, respectively form the initial parent material. In both cases this is a significant improvement over the untreated samples.

When considering the data obtained for the austenitic specimens, it can be seen that whilst both nitriding and carburising modifications reduce the amount of wear evident in the parent material specimen. In turn the nitrided specimen blades have shown a greater reduction in the wear experienced than the carburised samples. Similar evidence is seen in the martensitic specimens, with nitriding resulting in a greater improvement in the wear resistance of the specimens.

From post wear examination of the replica blades, using SEM characterisation, the wear mechanisms which are acting during the simulation testing have been determined. From the scratches which have formed on the surface of the edge it can be seen, figure 29-34 that the predominant wear mechanism which is acting during simulation testing is abrasive wear, with unidirectional scratches, produced as a result of contact between the blade and the counter-face material. Scratches seen in figure 29-34 are likely formed as a result of the removal of material from the PP counter-face material, during contact with the harder surface of the stainless steel blades. Particles removed from the PP surface become trapped

as debris between the two surfaces and during the sliding process, the result being the formation of the aforementioned scratches on the surface of the blade.

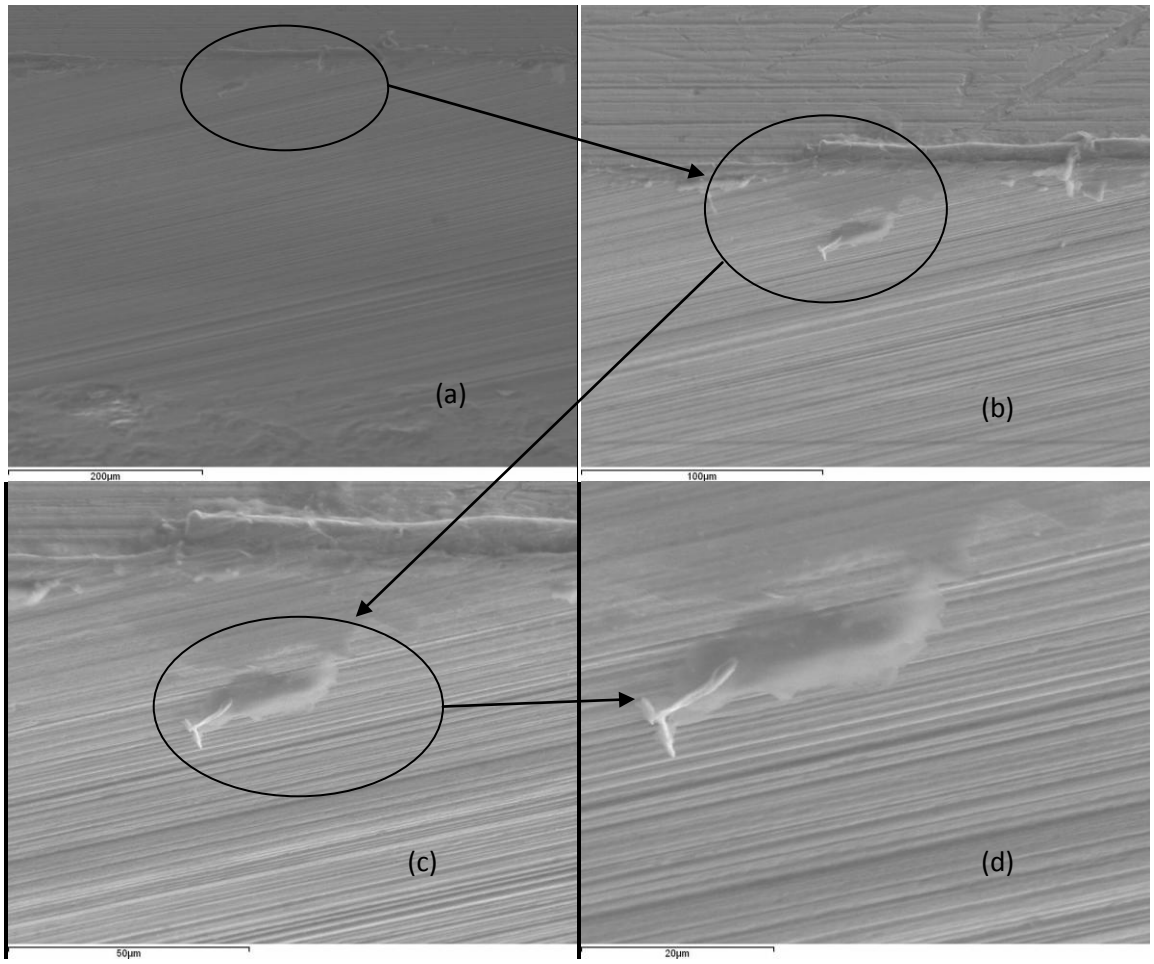

Figure 29 AISI 316 Untreated replica blade edges following wear simulation testing

Following examination of the wear tracks on the blade samples it is possible to determine the following information regarding the different materials and modification techniques. When examining the untreated blades; figure 29-34, it can be seen that the AISI 316 samples have seen a greater area of the surface undergo scratching than the AISI 420 samples, it is possible that this is due to the greater surface hardness which is inherently seen in the AISI 420 material. It can also be seen in figure 30 (d) that some material has collected on the blade, this is likely debris displaced from the counter-face material.

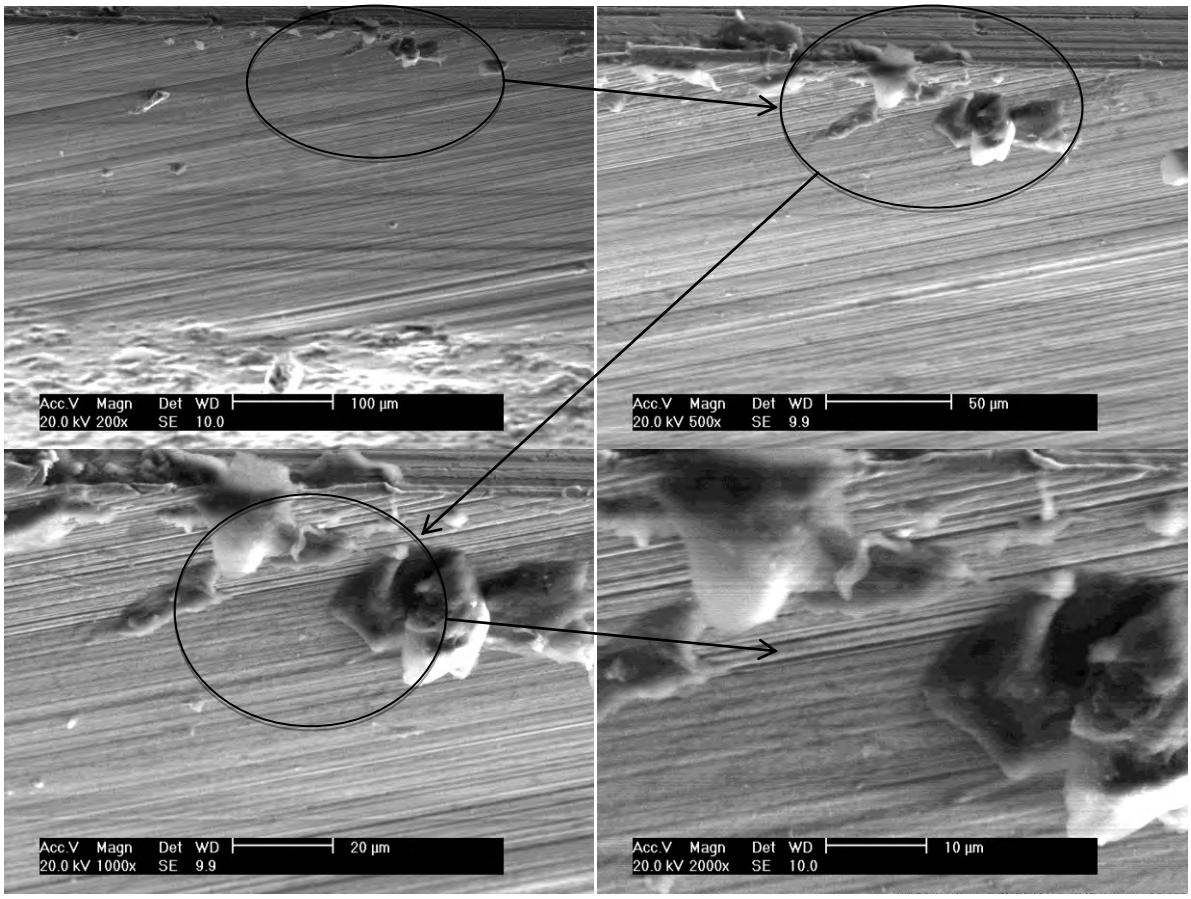

Figure 30 AISI 420 Untreated replica blade edges following wear simulation testing

Carburised blade edges, exhibit a similar wear tracks to those seen in the untreated samples, however, there are several differences which are made evident following SEM characterisation. It can be seen that the surface area of the blade edge which has been subjected to wear is significantly reduced in both the AISI 316 and the AISI 420 carburised blades figure 31 and figure 32 respectively, when compared to those seen in their respective untreated blade samples. Furthermore it can be seen that whilst the scratches remain largely unidirectional for the carburised specimens, they are much less severe than those exhibited in the untreated samples. Edge regions in the carburised samples also contain some material debris which has been removed from the surface of the counter-face material. There are equally some differences between the two carburised materials, the AISI

420 samples exhibit a smaller worn region, than that seen in the AISI 316 samples, however, the morphology of the track remains almost identical in both of the materials.

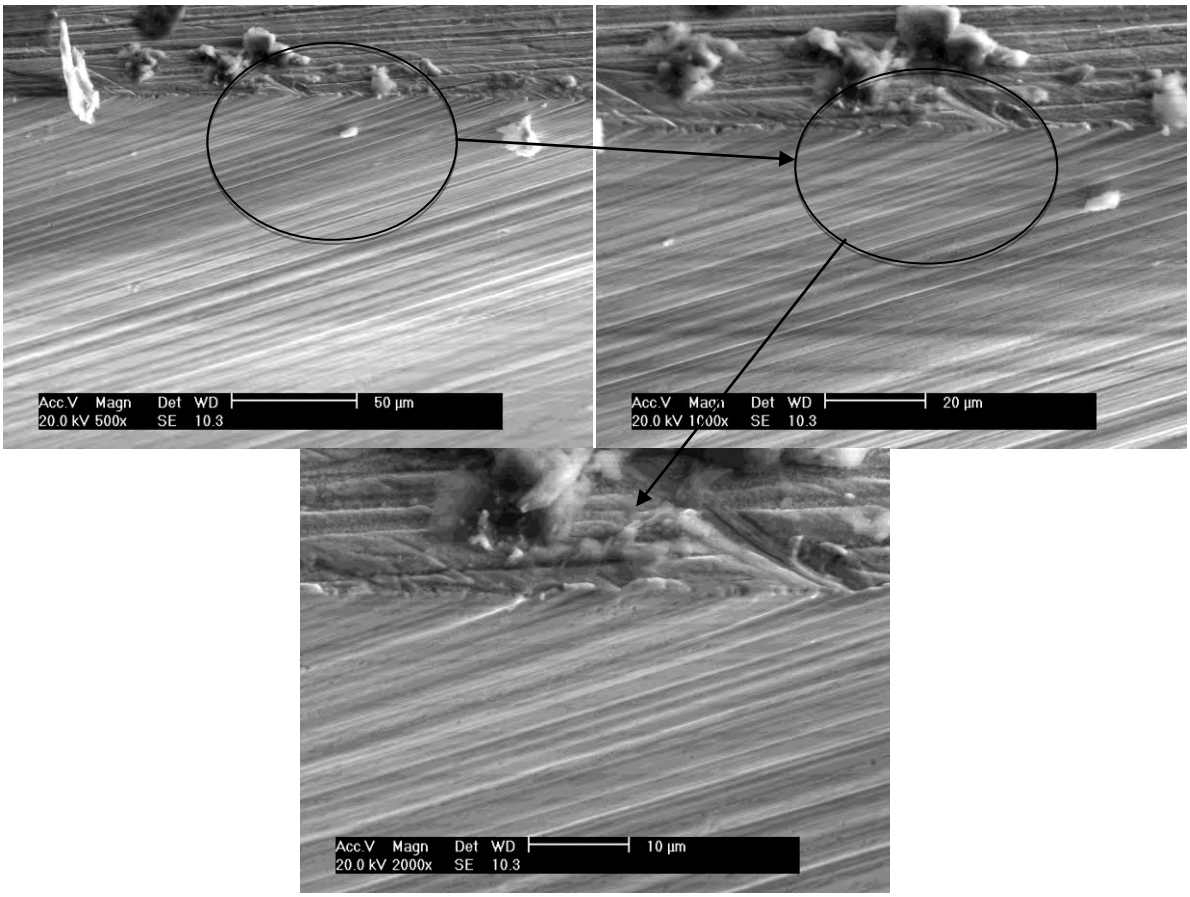

Figure 31 AISI 316 Carburised Replica blade edges following wear simulation testing

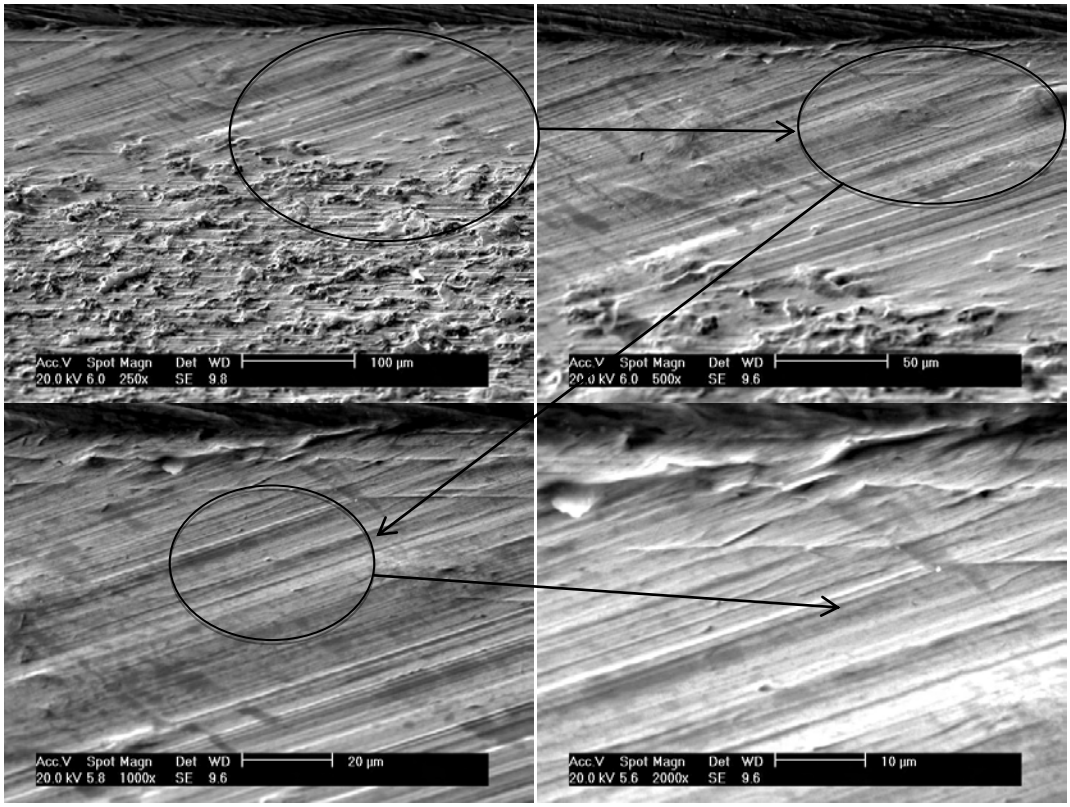

Figure 32 AISI 316 Nitrided Replica blade edge following wear simulation testing

When comparing the untreated blade wear tracks with those seen in the nitrided samples figure 33 and figure 34, it can be seen that whilst the scratches in the modified samples remain unidirectional there are several major differences which are evident. It is possible to see that the area which is covered by the wear track is greatly reduced in the nitrided samples; it is also possible to see that the scratches seen in the nitrided samples are much less pronounced than in the untreated sample blades. It is further possible to make a comparison between the AISI 316 and AISI 420 nitrided samples, with some differences to be seen between them respectively. However, in both cases there are examples of some adhesive wear occurring, along with the predominant abrasive mechanism. It can be seen that the AISI 420 samples exhibit a much smoother wear track, with fewer examples of adhesive spalling to be seen.

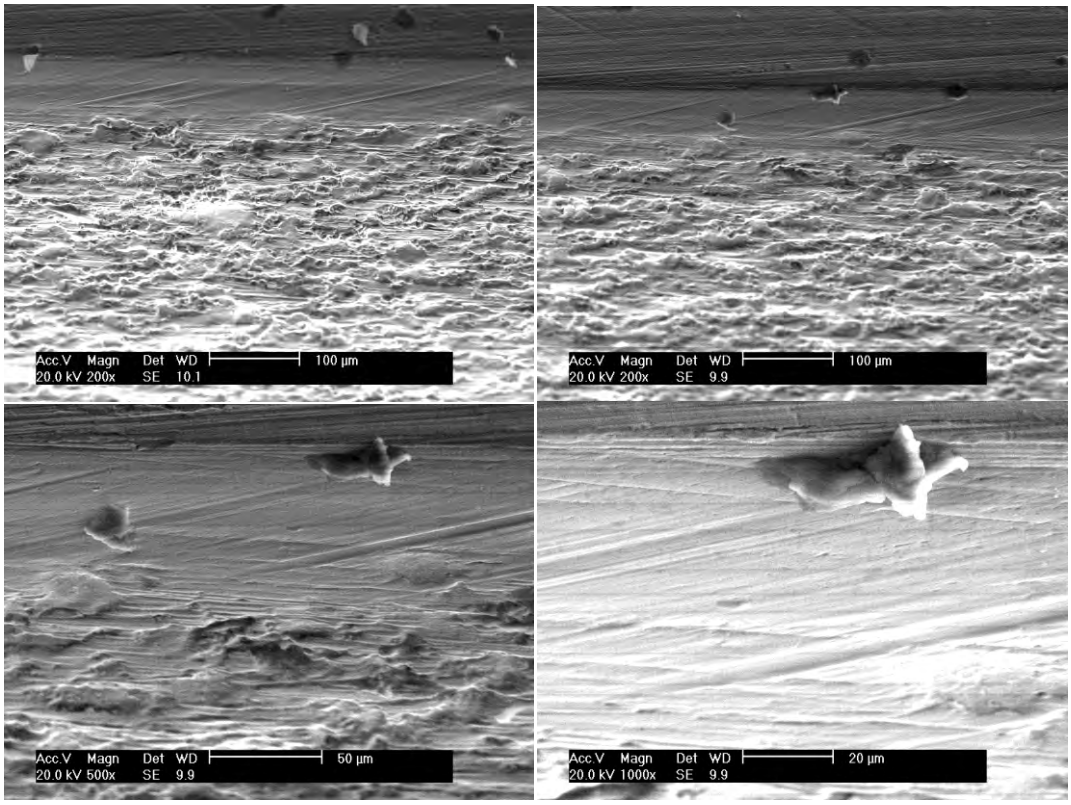

Figure 33 AISI 420 Carburised Replica blade edge following wear simulation testing

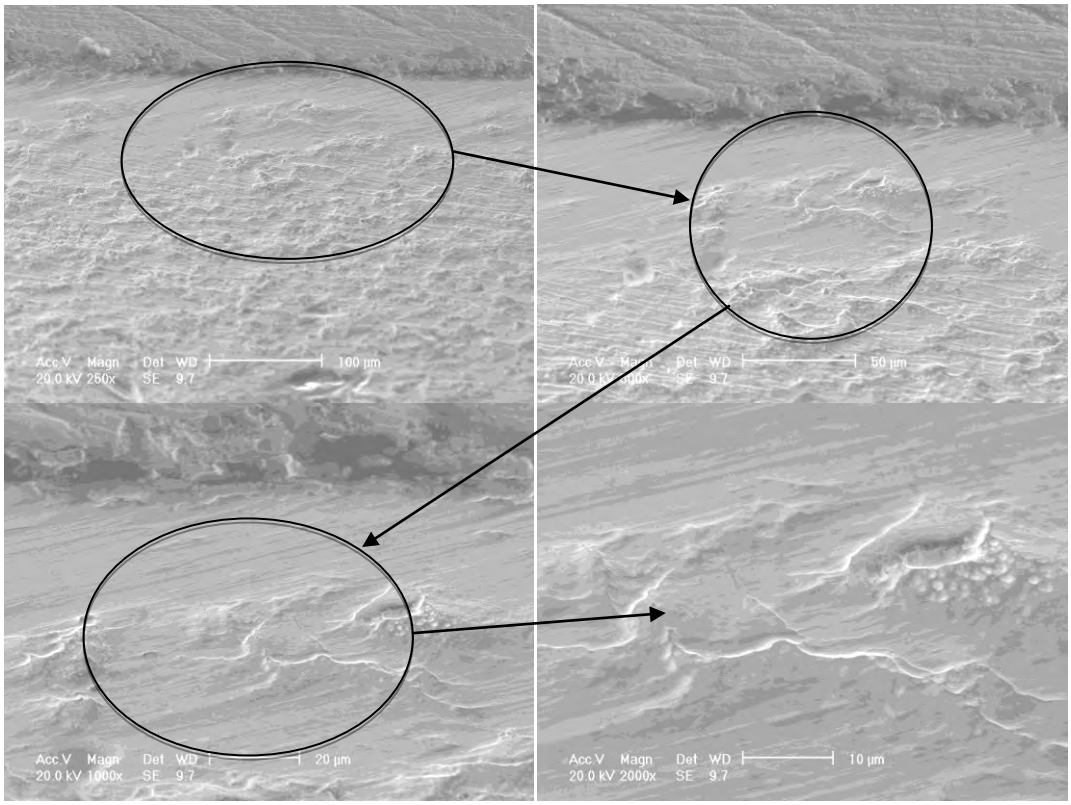

Figure 34 AISI 420 Carburised Replica blade edge following wear simulation testing

4.2.4 Friction

During simulation testing friction was measured during the blade sliding. Results from friction testing can be seen in figure 35-37, for untreated, carburised and nitrided replica blades. Comparing the friction experienced by the untreated samples, figure 35, during testing, it was seen that profiles are similar for both the AISI 316 and the AISI 420 replica blades, with an initial increase in friction through the first 1000 cycles, from 9 N to 17 N for AISI 316, and 9 N to 16 N for AISI 420. This initial increase is followed by a constant level of friction through the remainder of the sliding simulation cycle. It can also be seen that the AISI 420 sample is exposed to a lower level of friction than the AISI 316 sample; this is due to its higher surface hardness value.

When considering the carburised samples, figure 36, it can be seen that again trends exhibited are similar for both materials. However, as opposed to the profile seen for the untreated sample carburised samples are exposed to lower friction 10-12 N for AISI 316 and 6-9 N for AISI420. Throughout the test period the trend is for the friction to increase gradually up to the maximum value. Lower friction is associated with the improvement in surface hardness of both materials, and the trend towards gradual increase in friction can be attributed to removal of the treated layer as a result of the sliding.

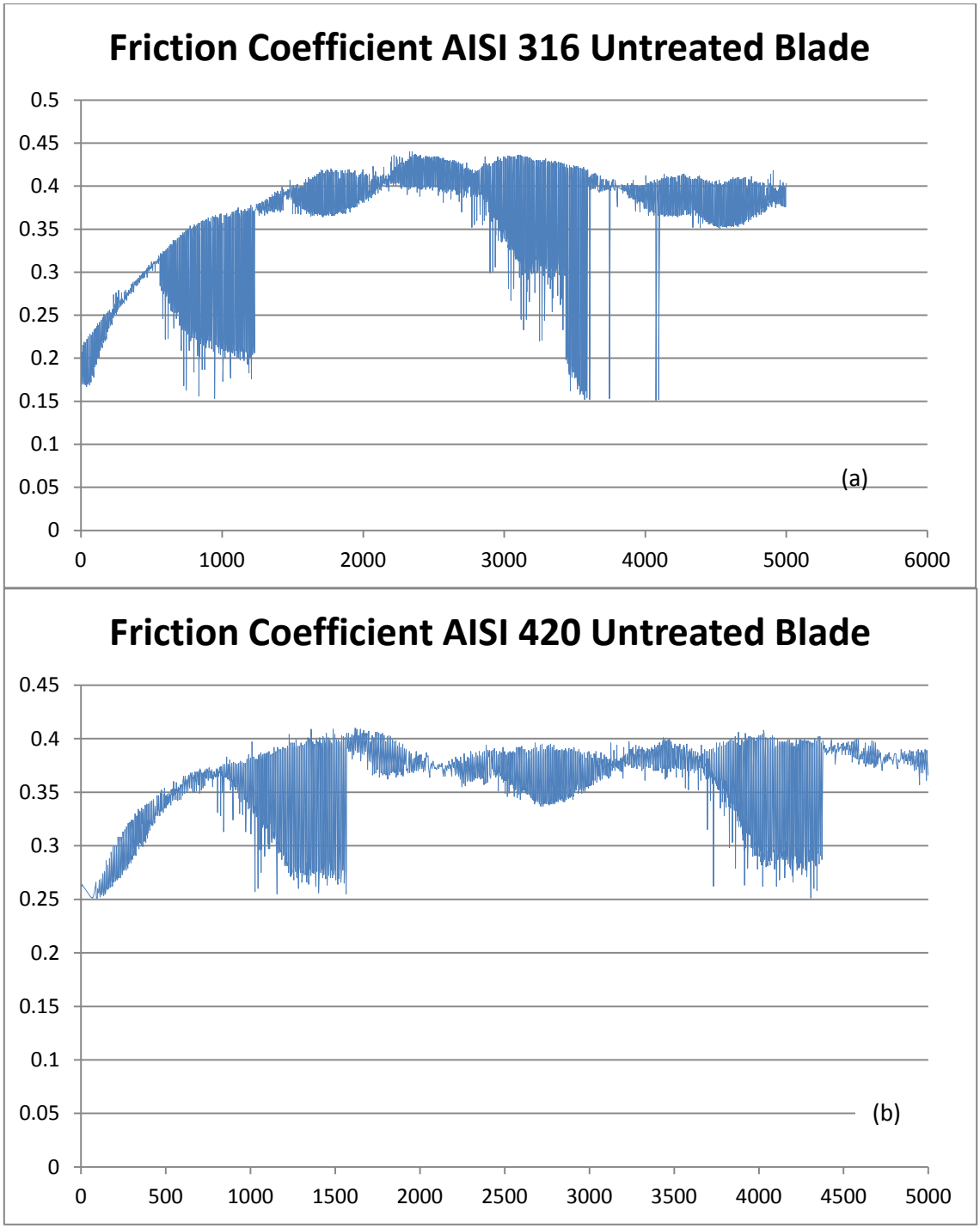

Figure 35 Untreated replica blade samples, measured friction during simulation testing (a) AISI 316, (b) AISI 420

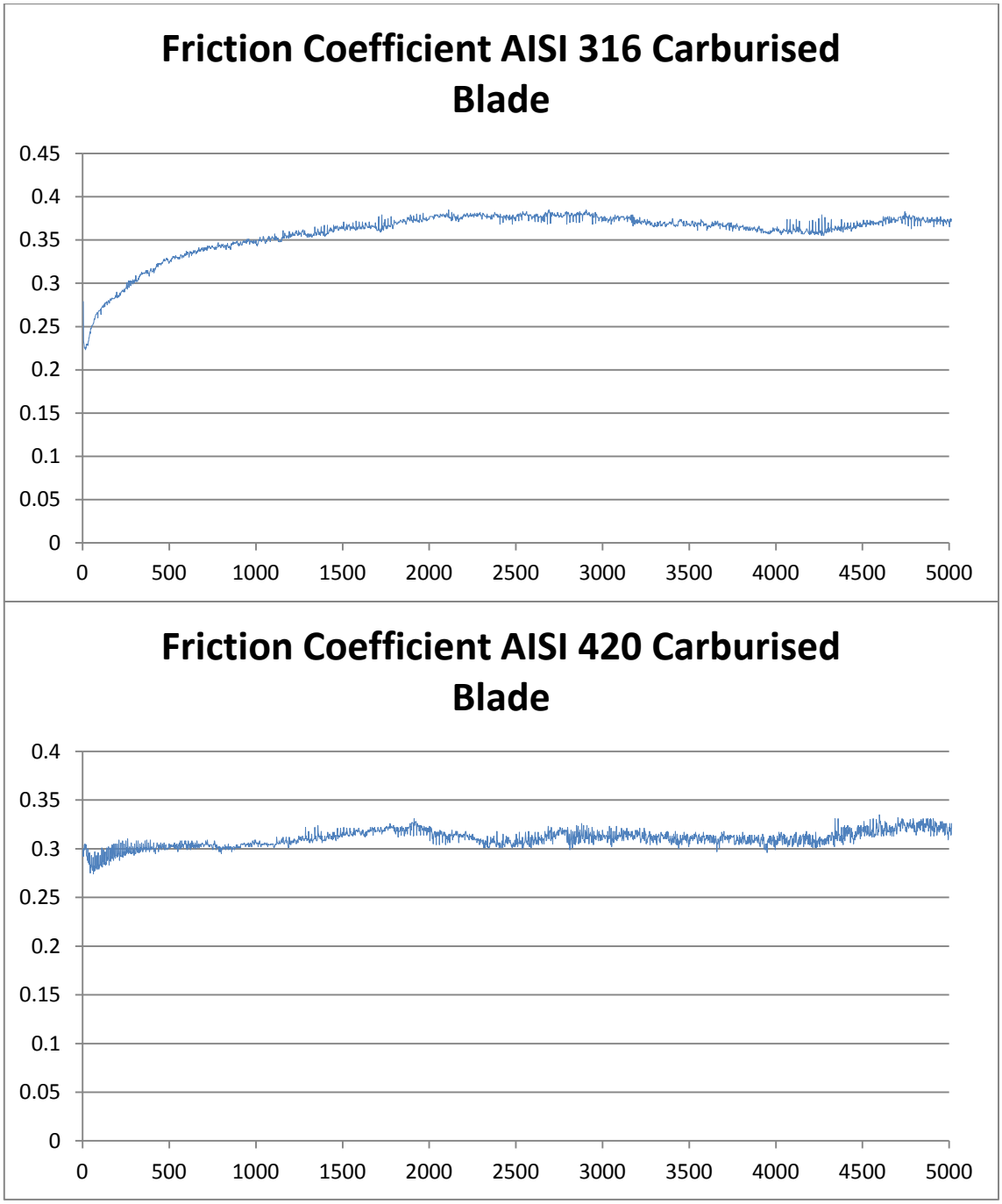

Figure 36 Carburised replica blade samples, measured friction during simulation testing, (a) AISI 316, (b) AISI 420

Nitrided AISI 316 samples, figure 37 (a), show a similar trend to the carburised samples with a gradual increase throughout the test period as the modified layer is slowly worn away. However, initial friction is lower at 6 N, the increase in friction is more pronounced than in

the carburised sample due to the fact that the nitrogen does not diffuse as deeply though the parent material as carbon. Nitrided AISI 420 samples, figure 37 (b) show a different trend with a constant friction, 6 N, being experienced through the entire 5000 cycles. This is likely due to the fact that the modified layer is more resistant to removal owing to its higher hardness. Higher hardness means a smoother surface finish which produces less rough edges to generate friction between the blade edge and the counter-face material.

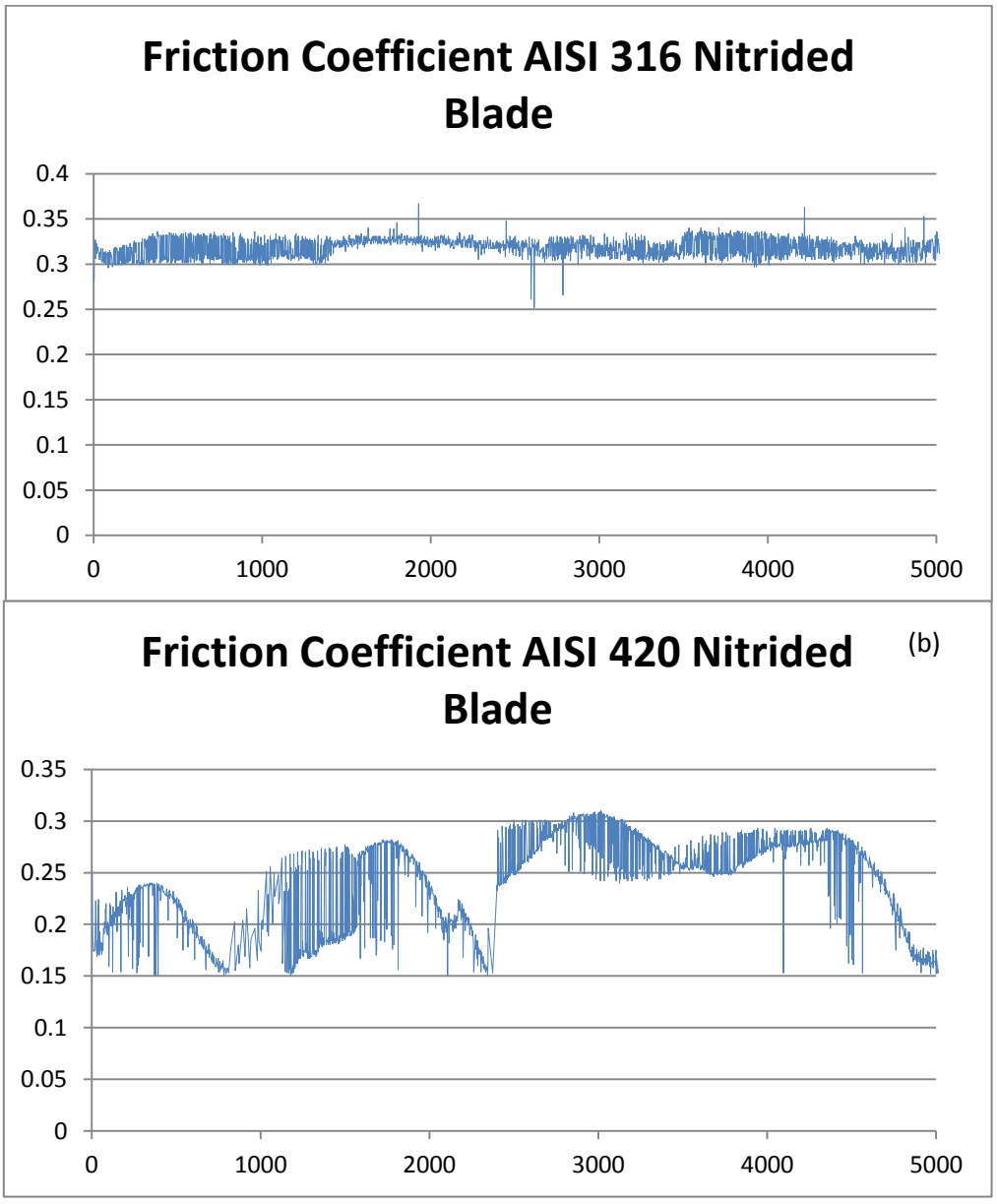

Figure 37 Nitrided replica blade samples, measured friction during simulation testing, (a) AISI 316, (b) AISI 420

5 Discussion

When considering the results obtained during the study, it is important to consider the meaning of some of the findings. With regards to the previous research in the area of surface modification of stainless steels, results obtained as a course of this study are in agreement with studies carried out into the benefits of low temperature surface modifications, for a variety of other applications.

Findings in the study, confirm that nitriding, carburising and carbo-nitriding modifications, can provide a marked improvement in the bulk properties of the parent material. This improvement has been observed in the surface hardness properties, of stainless steels, as well as an improvement in the hardness of the near surface region. During the course of this study a similar improvement has been seen in both the disc samples, and in the replica blade samples. From the experiments during this study it has been determined that whilst nitriding produces a greater improvement in the hardness of the surface region, carburising produces a greater effective depth of diffusion of the modified layer. Similarly to previously documented results, the modified region which produces this improvement in the surface properties of the material has been brought about as a result of changes in the surface micro-structure. These changes, are likely due to the super-saturation of the surface and near surface region. Previous work on the characterisation of S-phase in austenitic stainless steels suggests that this is likely a γ_N phase[11, 83], often referred to as expanded austenite.

Changes in surface micro-structure, are seen in the austenitic samples in the form of a smooth “white (featureless)” region, under optical observation. In the martensitc sample’s as with previous research a change in the structure of the surface region can also be seen ,

however as opposed to observing a smooth white layer, a diffusion region is formed which exhibits a different micro-structure to that seen in the parent material.

A comparison between the GDOES plots and the cross-sectional micro-hardness figures has been made in order to further establish a comparison of effective diffusion depth of the modification. Figure 38-41, demonstrate that the diffusion profiles and the cross-sectional hardness profiles show similar plots, which indicates that the values obtained for the effective diffusion depth of the modification are consistent. A 2007 study by Buhagiar *et al.*[84], characterising the effective diffusion depths of nitriding, carburising and carbo-nitriding treatments in medical grade austenitic stainless steels, showed similar trends to those observed in this study.

When considering reason's for the differences in wear tracks observed on the blade samples there are several possibilities. When comparing the tracks on the untreated and treated blades, the predominant reason behind the reduction in the scratched area, it is likely that the driving factor is the improved surface hardness following modification. However, it is also possible to attribute some of the improvement to the reduced surface roughness which arises in the modified samples, thus reducing the susceptibility of the surface to attack by wear mechanisms.

When considering the differences seen in the AISI 316 and the AISI 420 nitrided samples, it is not so simple to suggest possible sources. It is not possible to attribute differences to surface hardness, as both exhibited similar surface hardness values following modification. However, it is possible that differences could be attributed to differences in the way in which the modified near surface region is formed, that is to say the s-phase layer of expanded austenite in the AISI 316 samples, and a hardened diffusion zone in the AISI 420

samples. It is possible that the way in which the bonding occurs in the different modified layer may affect the way in which wear mechanism act during the simulation testing.

During the study several further interesting pieces have data have been discovered which further support the results previously outlined in the results section. This has been seen during examination of the wear tracks on the synthetic PP counter-face material. During this examination, it has emerged that the wear tracks left by the nitrided samples are seen to be leave a smoother groove in the surface of the PP, there is also less deposited worn material to be found in the same wear tracks. It can also be seen that the same nitrided samples, have left a much deeper wear track on the counter-face surface than the untreated and the carburised samples. The carburised samples, have left a smoother wear track in turn than the untreated samples, these tracks were also seen to be deeper than the untreated specimen tracks.

It is likely that the above observations can be related back to the surface hardness of the blade specimens. It follows that the hardest surface will be that which leaves the deepest groove in the counter-face material, with the least displacement of material from the specimen surface during the wear process. Thus as the nitrided samples exhibit the highest surface hardness during the characterisation testing, it logically follows that these are the samples that would leave the deepest and smoothest wear tracks in the PP counter-face.

Considering the results obtained during sliding wear and friction testing, it has been observed that there is good correlation between the samples which showed good improvements in wear resistance and those which showed low coefficient of friction during the sliding. This is in agreement with the observations from the surface hardness and wear

resistance data, with a corresponding drop in the coefficient of friction during sliding, and samples which exhibited an increased surface hardness.

Figure 43 shows profile measurements of the wear tracks left on the synthetic ice counter-face material following testing. It can be seen that the nitrided sample has produced the deepest track, when compared to those left by the carburised and untreated samples. It can also be seen from the optical images, figure 42 that the nitride samples have left a significantly smaller amount of deposited material on the synthetic ice following testing.

EDX examination of debris particles, figure 44, found in the wear track in the blade edges, indicate that they appear to be material which has been removed from the synthetic ice counter-face. It can be seen that the particle contains traces of oxygen, silicon and elevated levels of carbon, which are three of the major component elements present in the synthetic ice material used as a counter-face during wear simulation. However, composition of the wear track with no debris material reveals no trace of oxygen or silicon, and normal levels of carbon expected in the parent bulk material.

Corrosion behaviour of the stainless steels, both prior to and following modifications, was not extensive but initial indication is in agreement with results seen in a study by Li and Bell[65], where plasma nitriding of AISI 410 martensitic stainless steel, exhibited a similar trend for improved corrosion resistance following immersion in 3.5 .% NaCl. The results obtained in this study whilst demonstrating a slight improvement in the resistance to corrosion of the bulk material, must be considered as indicative and not as a fully confirmed. Owing to the fact that only single samples were tested for each condition.

The difference in resistance between the lower temperature treatments and higher temperature treatments is likely due to the decreased level of Cr in grains following exposure to higher temperture treatments. Above a critical temperature, the Cr will migrate towards the grain boundaries, where it will precipitate to form carbide rich regions, leaving a Cr depleted region the centre of the grain whic is more susceptible to corrosin.

When considering the results obtained during the course of this study it is important to note several important pieces of information. Initially, that all testing carried out for the purposes of this research has been carried out on a scaled down basis. It must also be taken into consideration that all testing has been carried out in an environment which is different to that in which ice skating truly occurs, that is to say that whilst temperature has been controlled during testing, all testing has occurred at room temperature, as opposed to being at carried out at near $0^{o}C$ where ice truly forms. It is also important to remember that whilst testing has been carried out using synthetic ice designed to replicate a true ice environment, it will never be possible to produce results which are 100% accurate unless testing is carried out in a true environment against real ice.

It is important to note that during this study owing to time constraints it has not been possible to apply the use of carbo-nitriding technologies to the replica blades, however, during testing of the dummy disc samples, it was determined that this may well prove to be an extremely effective method for modifying the surface of samples. This might prove to be an interesting area to explore in future work.

6 Conclusions

1. Plasma Surface modification techniques, carburising, nitriding and carbo-nitriding, greatly improve the surface hardness of the untreated bulk materials, AISI 316 and AISI 420 stainless steels, with nitriding proving the most effective.

2. Carburising, produces a greater effective diffusion depth over the entire temperature range considered during the study.

3. Treatments occurring at temperatures of 500^{o}C or below for both nitriding and carburising showed the greatest improvement in all areas related to tribological properties.

4. This improvement in surface hardness, is due to the formation of a modified layer, a typical S-phase region in the AISI 316 samples, and the formation of a s-phase compound layer in the AISI 420 samples.

5. Surface modification of replica ice skate blades, has shown an improvement in resistance to wear during simulation sliding, as well as an improvement in resistance to impact, seen as a result of hardness testing.

It can be said that through the use of surface modification techniques, such as nitriding and carburising, the tribological properties of stainless steels for potential use in ice skate blades can be greatly improved.

7 Future Work

Concerning the direction in which the research carried out during this study should be heading, there are several avenues which could be pursued in the future. Initially, the suggestion would be to carry out comparative wear simulation testing using a more true to life environment. That is to say by carrying out wear testing with scale sample blades against real ice, in a temperature controlled environment. Following this it should be the goal to apply this method to full scale blades, and review success of the modification, in a real life situation by measuring wear of the blade, following use by an ice skater. This will enable experimental data to be obtained concerning damage to the blade, as well as for the skater testing the technology to provide feedback as to any performance related changes which they may feel.

Due to the time constraints placed upon this study it has not been possible to make use of the carbo-nitriding plasma surface alloying technique on the replica blade samples. It is important for any future studies to involve the use of this technology, as it has been proven that carbo-nitriding can produce the greatest improvement in surface hardness of the the commonly applied surface alloying techniques.

Further attention can also be paid to sliding applications in an environment containing a surface film of moisture to further replicate conditions which are likely to be experienced in actual application areas.

It may further be possible to examine the use of surface modification technologies, with other materials, which have previously not been considered as an option for use in this specific application. This may be due to certain poor inherent properties of the bulk material

which currently removes them as a viable option. But through the use of technologies examined during this study it may be possible to consider them.

Furthermore it is possible to apply the technologies and results found during this study in other similar applications, for example in ski edges, bobsleigh runners and other sliding contact applications, where a materials tribological properties are a major driving issues during the design and selection process.

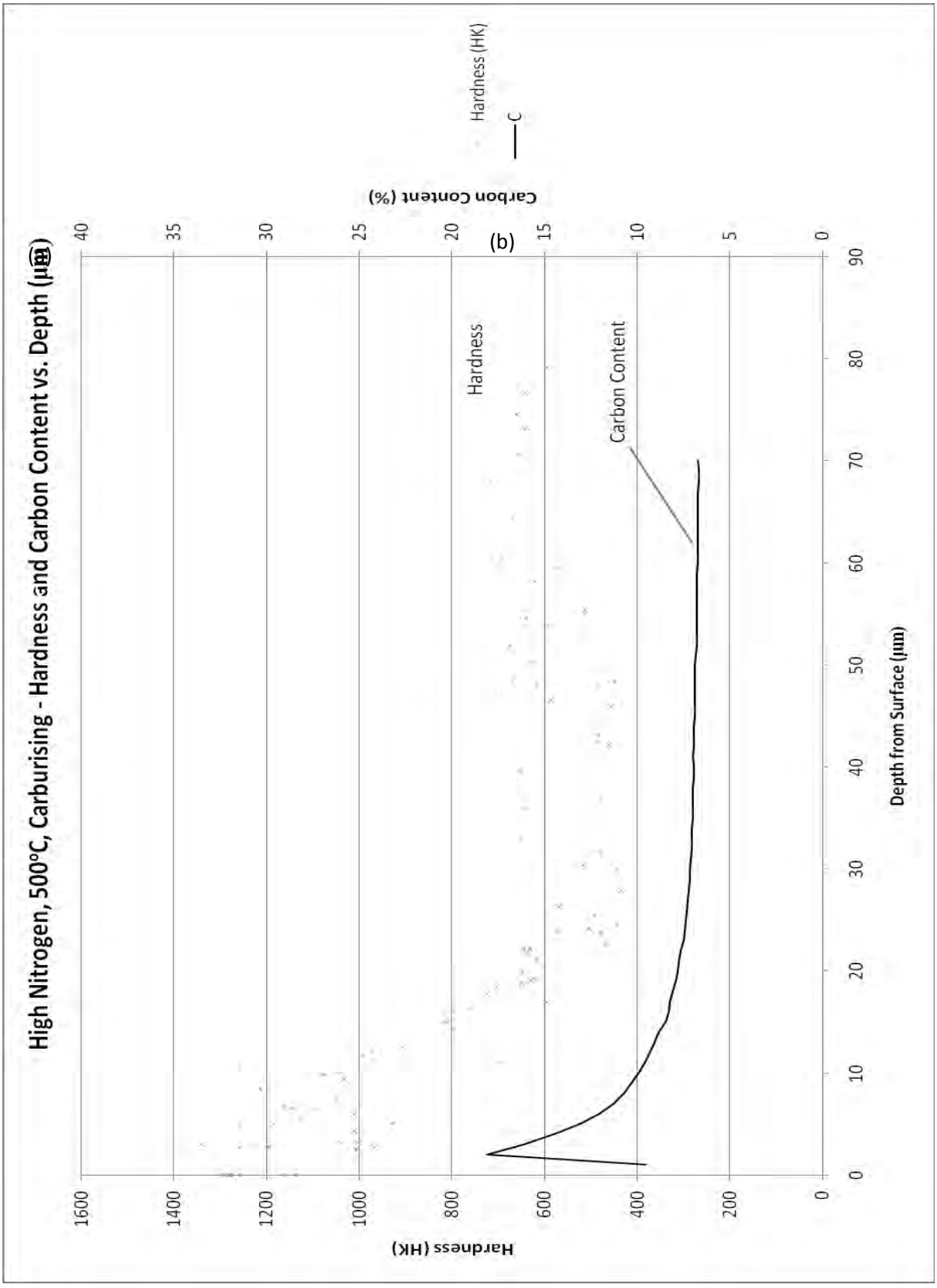

Figure 38 Cross-sectional Mirco-hardness against GDOES diffusion profiles for AISI 316 Carburised disc sample

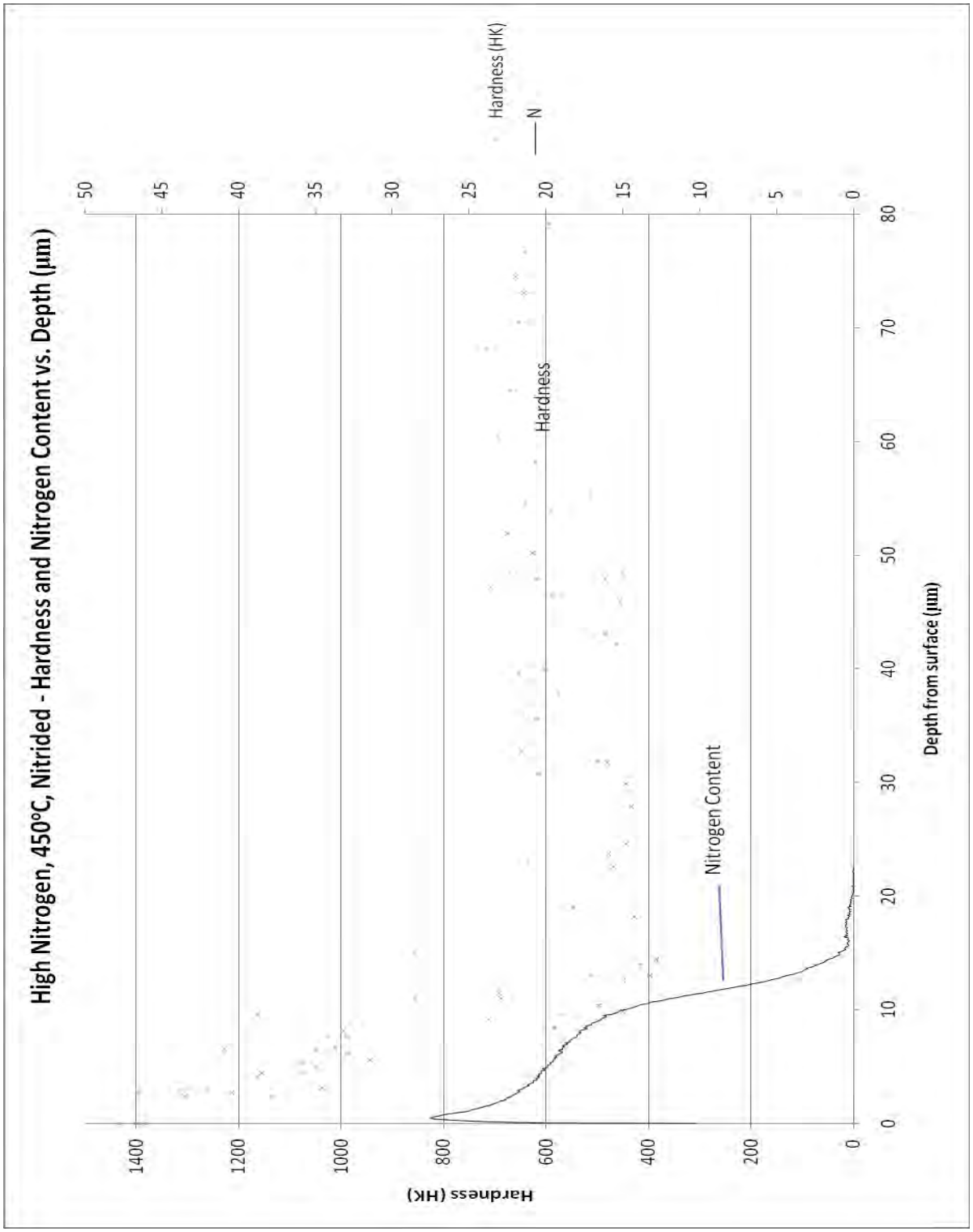

Figure 39 – Cross-sectional Mirco-hardness against GDOES diffusion profiles for AISI 316 Nitrided disc sample

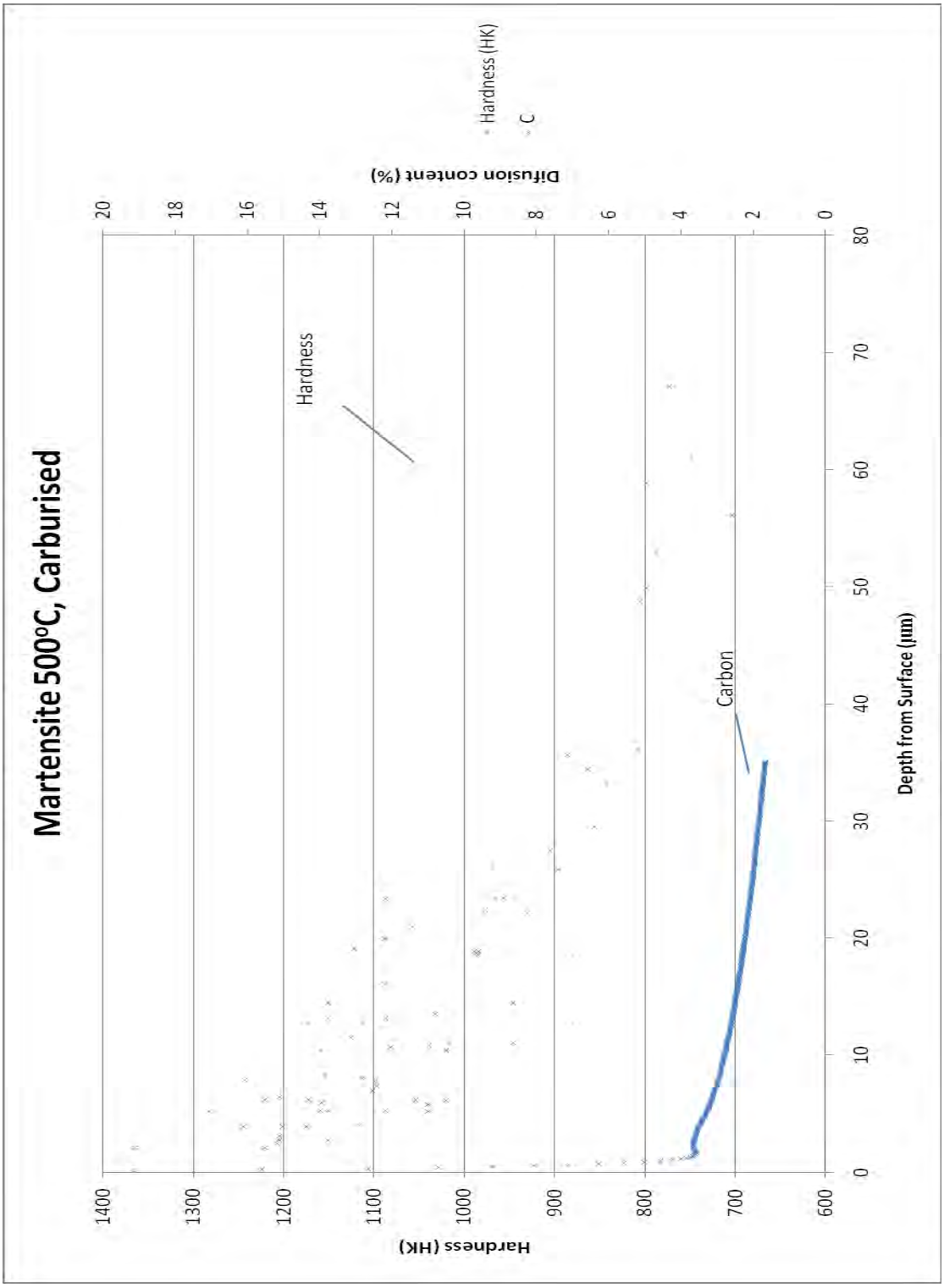

Figure 40 - Cross-sectional Mirco-hardness against GDOES diffusion profiles for AISI 420 Carburised disc sample

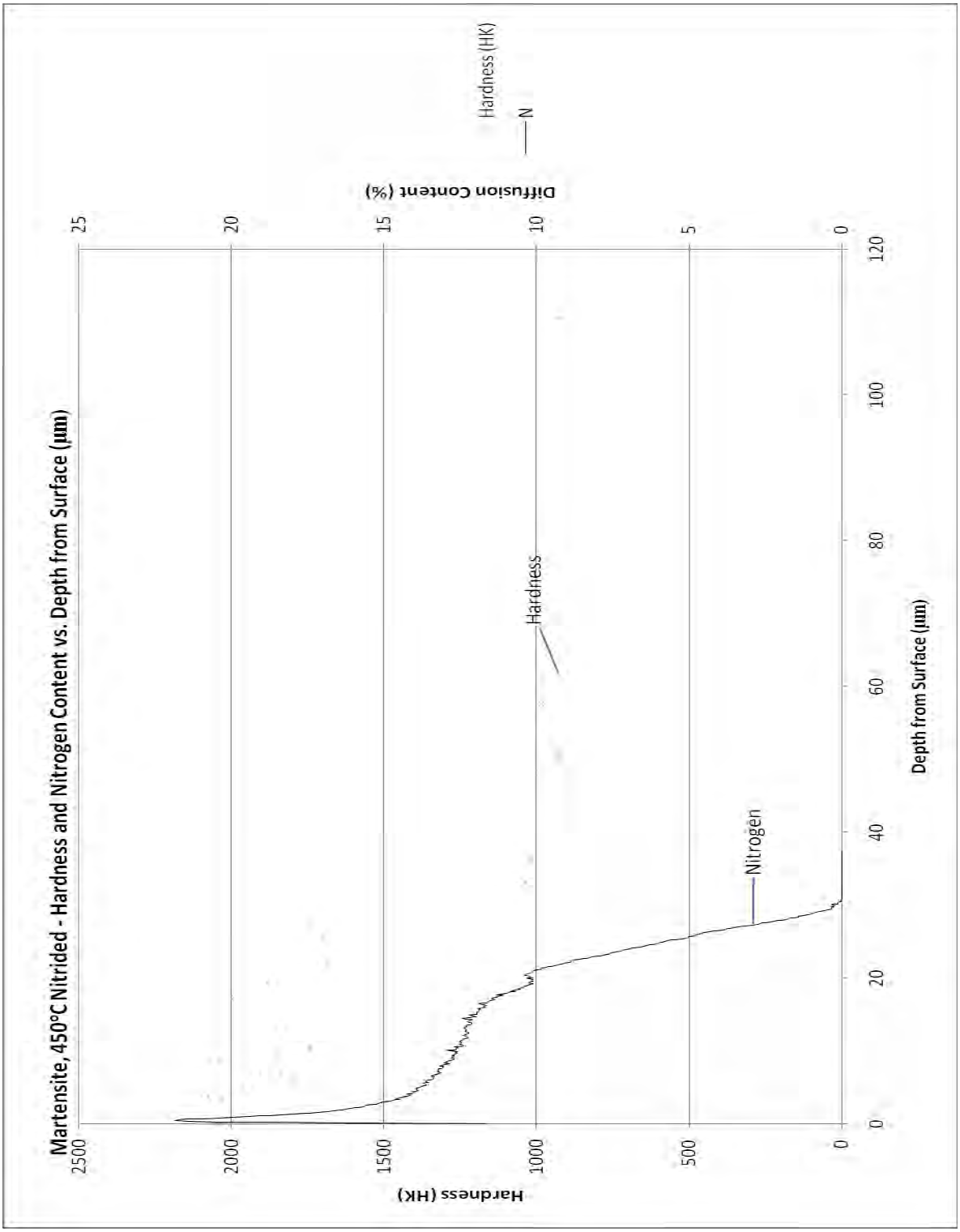

Figure 41 - Cross-sectional Mirco-hardness against GDOES diffusion profiles for AISI 420 Nitrided

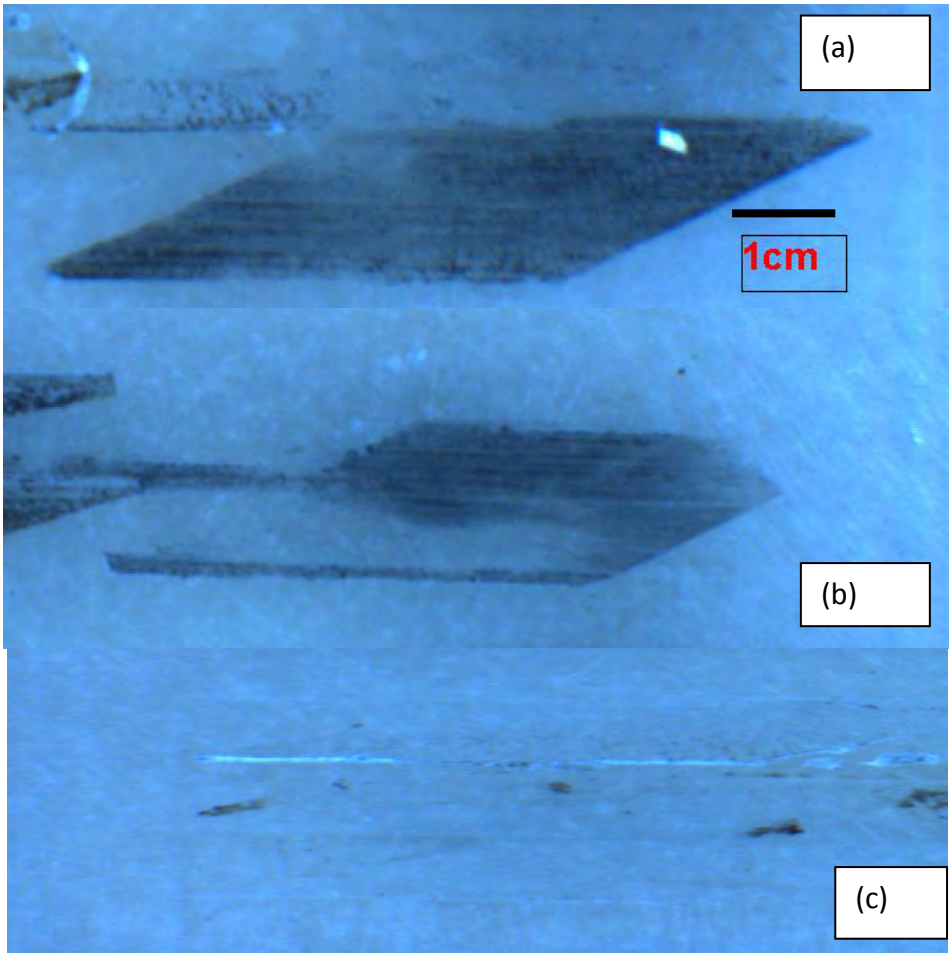

Figure 42 – Wear tracks in synthetic ice surface following sliding wear testing (a) Untreated, (b) Carburised (c) Nitrided blades

Figure 43 – Surface Roughness profiles, PP synthetic ice counter-face wear tracks for (a) AISI316 Untreated, (b) AISI 316 Carburised, (c) AISI 316 Nitrided following sliding simulation testing

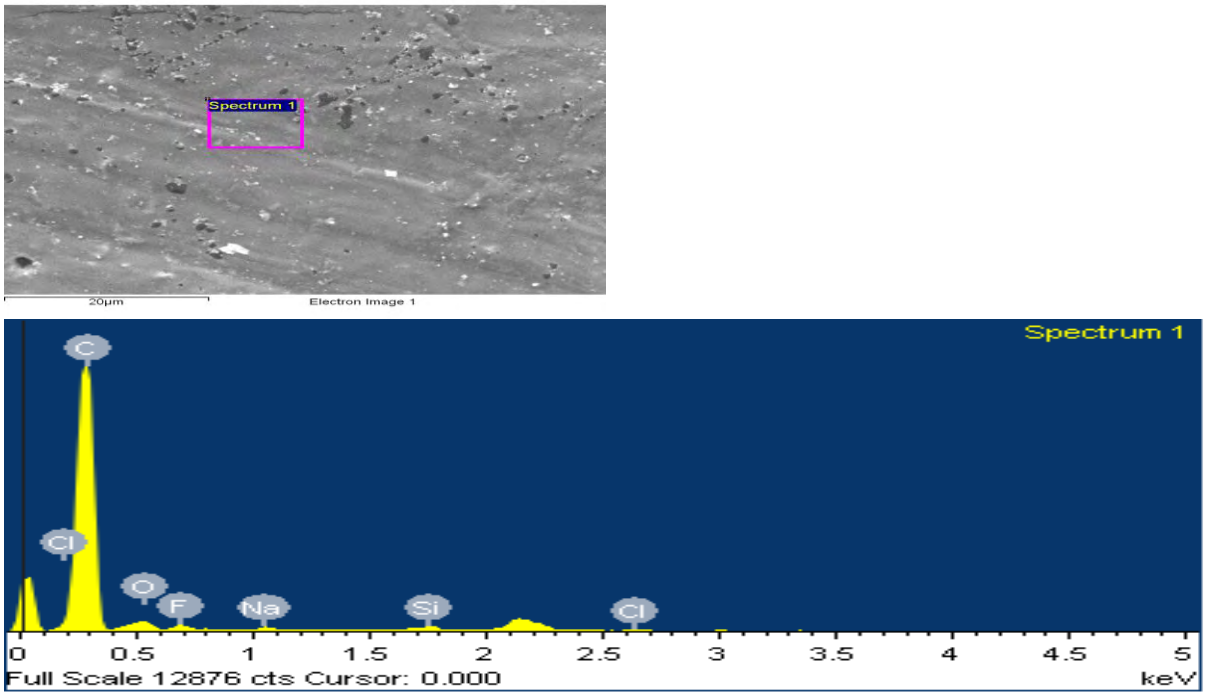

Figure 44 – Analysis of synthetic ice counter-face surface debris following completion of sliding testing

8 Acknowledgements

I would like to thank several people for devoting a great deal of time and effort to helping me during the course of this study. Most notably Professor Hanshan Dong and Dr Jian Chen, without whom I would have been very much all at sea. They have provided guidance, training and advice whenever it was asked for, and their help has been invaluable.

I would also like to thank Mr Christopher Few for his help with regards to fabrication of the counterfeit ice substitute. I would also like to thank the other members of the surface engineering group, as well as Mr Paul Stanley for helping with microscopy training, and continued help throughout the project.

9 References

1. Publow, B., *Speed on Skates*. 1999: Human Kinetics. 345.
2. Bowden, F.P. and Hughes, T.P, *The Mechanism of Sliding on Ice and Snow.* Proceedings of the Royal Society of London. Series A, Mathematical and Physical Sciences, 1939. **172**(949): p. 280-298.
3. Li, C.X. and Bell, T., *Sliding wear properties of active screen plasma nitrided 316 austenitic stainless steel.* Wear, 2004. **256**(11-12): p. 1144-1152.
4. Horkheimer, D., *Improvements in Ice Skate Blade Performance through the use of PVD and CVD Plasma Hard Coatings*. 2007, University of MInnesota: Minnesota. p. 21.
5. Larisch, B., Brusky, U. and Spies, H.J., *Plasma nitriding of stainless steels at low temperatures.* Surface and Coatings Technology, 1999. **116-119**: p. 205-211.
6. Li, C.X., Georges, J. and Li, X.Y. , *Active screen plasma nitriding of austenitic stainless steel.* Surface Engineering, 2002. **18**: p. 453-457.
7. Menthe, E., Bulak, A., Olfe, J., Zimmermann, A. and Rie, K.T. *Improvement of the mechanical properties of austenitic stainless steel after plasma nitriding.* Surface and Coatings Technology, 2000. **133-134**: p. 259-263.
8. Bell, T., Y. Sun, and A. Suhadi, *Environmental and technical aspects of plasma nitrocarburising.* Vacuum, 2000. **59**(1): p. 14-23.
9. K.N. Strafford, R.C.S., I. Sare C. Subramanian, ed. *Surface Engineering: Process's and Applications*

1995, Technomic Publishing.

10. Rie, K.T., *Recent advances in plasma diffusion processes.* Surface and Coatings Technology, 1999. **112**(1-3): p. 56-62.
11. Liang, W., *Surface modification of AISI 304 austenitic stainless steel by plasma nitriding.* Applied Surface Science, 2003. **211**(1-4): p. 308-314.
12. Rolinski, E. *Effect of plasma nitriding temperature on the surface properties of austenitic stainless steel.* Surface Engineering, 1987. **3**(1): p. 35-40.
13. Carter, S. *How to Understand the History of Ice Skating*. 2009; Available from: http://www.howtodothings.com/sports-recreation/understand-the-history-of-ice-skating.
14. Lad, K. *History of Ice Skating*. 2009; Available from: http://www.buzzle.com/articles/history-of-ice-skating.html.
15. Federico, F. and M. Alberto E, *The first humans travelling on ice: an energy-saving strategy?* Biological Journal of the Linnean Society, 2008. **93**(1): p. 1-7.
16. Henry, J. *The History of Figure Skating*. 2007; Available from: http://www.catalogs.com/info/sports/history-of-figure-skating.html.
17. Fitzpatrick, J. *Ice Hockey History Time Line - A Quick Look at Ice Hockey History*. 2009; Available from: http://proicehockey.about.com/od/history/a/history_timelin.htm.
18. Kuper, G.H. and E. Sterken, *Endurance in speed skating: The development of world records.* European Journal of Operational Research, 2003. **148**(2): p. 293-301.
19. Koning, R.H., *Home advantage in speed skating: Evidence from individual data.* Journal of Sports Sciences, 2005. **23**(4): p. 417 - 427.
20. Bellis, M. *Ice Skates*. 2009; Available from: http://inventors.about.com/library/inventors/bliceskates.htm.
21. Tek, B. *The Radius*. 2011 [cited 2011 17/08/2011]; Available from: http://www.blade-tek.com/theRadius.html.
22. Company, W.M. *Learning About Radius*. 1996 [cited 2011 17/08/2011]; Available from: http://www.wissota.com/toppage.htm.

23. Everglides. *How Ice Skates Work*. Available from: http://www.everglides.co.uk/html/about_ice_skates.html.
24. McNulty, M.F. *Ice Skates*. 1996; Available from: http://www.enotes.com/how-products-encyclopedia/ice-skates.
25. Saint, N. *How Innovation has changed the Winter Olympics*. 2010; Available from: http://www.google.co.uk/imgres?imgurl=http://static.businessinsider.com/image/4b83d19c0000000000c36873-400-300/speed-skating-now.jpg&imgrefurl=http://shine.yahoo.com/channel/life/how-innovation-has-changed-the-winter-olympics-852971/&usg=__aWnWFfWgyttbLHt-zEgxfI2-jXY=&h=300&w=399&sz=14&hl=en&start=13&um=1&itbs=1&tbnid=8P1D8xEMfkHdQM:&tbnh=93&tbnw=124&prev=/images%3Fq%3Dclap%2Bskates%26um%3D1%26hl%3Den%26safe%3Dactive%26sa%3DN%26tbs%3Disch:1.
26. Sanderson, A. *The Many Dimensions of Competitive Balance.* Journal of Sports Economics, 2002. **3**: p. 204-228.
27. Houdijk, H.A.N., J.J. de Koning, G. de Groot, M.F. Bobbert, and G.J.A.N.v.I. Schenau, *Push-off mechanics in speed skating with conventional skates and klapskates.* Medicine & Science in Sports & Exercise, 2000. **32**(3): p. 635-641.
28. de Koning, J.J, H.H., G. de Groot, M.F. Bobberet, *From biomechanical theory to application in top sports: the Klapskate story.* Journal of Biomechanics, 2000. **33**(10): p. 1225-1229.
29. Maenoa, N. and M. Arakawa, *Adhesion shear theory of ice friction at low sliding velocities, combined with ice sintering.* Journal of Applied Physics, 2004. **95**(1): p. 134-139 %U http://ci.nii.ac.jp/naid/120000955325/en/.
30. de Koning, J.J G.d.G., G.J. van Ingen Schenau, *Ice friction during speed skating.* Journal of Biomechanics, 1992. **25**(6): p. 565-571.
31. Fowler, A.J. and A. Bejan, *Contact melting during sliding on ice.* International Journal of Heat and Mass Transfer, 1993. **36**(5): p. 1171-1179.
32. Timco, G.W. and R.M.W. Frederking, *Experimental Investigations of the Behavior of Ice at the Contact Zone*, in *Studies in Applied Mechanics*, A.P.S. Selvadurai and M.J. Boulon, Editors. 1995, Elsevier. p. 35-55.
33. Colbeck, S.C., L. Najarian, and H.B. Smith, *Sliding temperatures of ice skates.* American Journal of Physics, 1997. **65**(6): p. 488-492.
34. Evans, D.C.B., J.F. Nye, and K.J. Cheeseman, *The Kinetic Friction of Ice.* Proceedings of the Royal Society of London. Series A, Mathematical and Physical Sciences, 1976. **347**(1651): p. 493-512.
35. Williams, J.A., *Wear and wear particles--some fundamentals.* Tribology International, 2005. **38**(10): p. 863-870.
36. Ducret, S., H. Zahouani, A. Midol, P. Lanteri, and T.G. Mathia, *Friction and abrasive wear of UHWMPE sliding on ice.* Wear, 2005. **258**(1-4): p. 26-31.
37. Farris, J.A.S. *Review of Paramount Figure Skating Blades*. 2009; Available from: http://figureskating.about.com/od/bootsandblades/gr/paramount.htm.
38. Skates, P. *Paramount Skates - Blades*. 2009; Available from: http://www.skatebladeperfection.com/blades.htm.
39. Marshall, P., *Austenitic Stainless Steels: Microstructure and Mechanical Properties*. 1984: Elsevier. 431.
40. AZoM™. *Stainless Steels - Introduction To The Grades And Families*. 2001; Available from: www.azom.com/Details.asp?ArticleID=470.
41. Davis, J.R., ed. *Stainless Steels (ASM Specialty Handbook)*. ed. A. International. Vol. 1. 1994, ASM International.
42. Kemppainen, J. *Stainless Steel – A New "Light Metal" for the Automotive Industry*. 2000; Available from: http://www.euro-inox.org/pdf/auto/Kemppainen_EN.pdf.

43. Dillon, C.P., *Corrosion Resistance of Stainless Steels*. 1995: Marcel Dekker, INC. 365.
44. Davis, J.R., *Stainless Steels (ASM Specialty Handbook)*. Illustrated ed, ed. H.C. ASM International. Vol. 1. 1994: ASM International. 577.
45. Voort, G.F.V., ed. *Metallography and MIcrostructures*. 1 ed. ASM Handbook, ed. A. International. Vol. 9. 2004, ASM International. 2733.
46. Schweitzer, P.A., *Encyclopedia of Corrosion Technology*. 2 ed. 2004: Marcel Dekker, INC. 675.
47. Alphonsa, I., A. Chainani, P.M. Raole, B. Ganguli, and P.I. John, *A study of martensitic stainless steel AISI 420 modified using plasma nitriding.* Surface and Coatings Technology, 2002. **150**(2-3): p. 263-268.
48. Cheng, Z., C.X. Li, H. Dong, and T. Bell, *Low temperature plasma nitrocarburising of AISI 316 austenitic stainless steel.* Surface and Coatings Technology, 2005. **191**(2-3): p. 195-200.
49. Borgioli, F., A. Fossati, E. Galvanetto, and T. Bacci, *Glow-discharge nitriding of AISI 316L austenitic stainless steel: influence of treatment temperature.* Surface and Coatings Technology, 2005. **200**(7): p. 2474-2480.
50. W.A. Glaeser, R.C.E., K.F. Dufrane & J.W Kannel, *Tribology: The Science of Combatting Wear*. 1981, Tribology Section Batelle: Columbus, Ohio. p. 52.
51. Batchelor, G.W.S.a.A.W., *Engineering Tribology*. 2 ed. 2000: Butterwoth Heinemann.
52. Association, B.S.S., *Corrosion Mechnisms in Stainless Steel*. 2007-2009, British Stainless Steel Association.
53. Wiezchon.T, B.T.a., *Surface Engineering of Metals: Priciples, Equipment, Technologies*. 1 ed. 1999: CRC Press. 605.
54. G.Dearnaley, *Ion Immplantation.* Nature, 1975. **256**: p. 701-705.
55. Bell, T., *Surface engineering of austenitic stainless steel.* Surface Engineering, 2002. **18**: p. 415-422.
56. Collins, G.A., R. Hutchings, K.T. Short, J. Tendys, X. Li, and M. Samandi, *Nitriding of austenitic stainless steel by plasma immersion ion implantation.* Surface and Coatings Technology, 1995. **74-75**(Part 1): p. 417-424.
57. Thierry, C., H. Huan, M. Grégory, T. Tony, W. Sylvain, and M. Henri, *Fundamental and Innovations in Plasma Assisted Diffusion of Nitrogen and Carbon in Austenitic Stainless Steels and Related Alloys.* Plasma Processes and Polymers, 2009. **6**(6-7): p. 401-409.
58. Sun, Y., *Enhancement in corrosion resistance of austenitic stainless steels by surface alloying with nitrogen and carbon.* Materials Letters, 2005. **59**(27): p. 3410-3413.
59. Leyland, A., D.B. Lewis, P.R. Stevensom, and A. Matthews, *Low temperature plasma diffusion treatment of stainless steels for improved wear resistance.* Surface and Coatings Technology, 1993. **62**(1-3): p. 608-617.
60. Li, X.Y., *Low Temperature Plasma Nitriding of 316 Stainless Steel - Nature of S Phase and Its Thermal Stability.* Surface Engineering, 2001. **17**: p. 147-152.
61. Boutonnet Kizling, M. and S.G. Järås, *A review of the use of plasma techniques in catalyst preparation and catalytic reactions.* Applied Catalysis A: General, 1996. **147**(1): p. 1-21.
62. Li, C.X. and T. Bell, *A comparative study of low temperature plasma nitriding, carburising and nitrocarburising of AISI 410 martensitic stainless steel.* Materials Science and Technology, 2007. **23**: p. 355-361.
63. Thomas, C. and A.J.S. Marcel, *On the crystallographic structure of S-phase.* 2004. **50**(1): p. 35-37.
64. Jiang, J.C. and E.I. Meletis, *Microstructure of the nitride layer of AISI 316 stainless steel produced by intensified plasma assisted processing.* Journal of Applied Physics, 2000. **88**(7): p. 4026-4031.
65. Li, C.X. and T. Bell, *Corrosion properties of active screen plasma nitrided 316 austenitic stainless steel.* Corrosion Science, 2004. **46**(6): p. 1527-1547.
66. Xu, X.L., L. Wang, Z.W. Yu, and Z.K. Hei, *Microstructural characterization of plasma nitrided austenitic stainless steel.* Surface and Coatings Technology, 2000. **132**(2-3): p. 270-274.

67. Marchev, K., C.V. Cooper, and B.C. Giessen, *Observation of a compound layer with very low friction coefficient in ion-nitrided martensitic 410 stainless steel.* Surface and Coatings Technology, 1998. **99**(3): p. 229-233.
68. Stagno, E., M.R. Pinasco, G. Palombarini, M.G. Ienco, and G.F. Bocchini, *Behaviour of sintered 410 low carbon steels towards ion nitriding.* Journal of Alloys and Compounds, 1997. **247**(1-2): p. 172-179.
69. Pinedo, C.E. and W.A. Monteiro, *On the kinetics of plasma nitriding a martensitic stainless steel type AISI 420.* Surface and Coatings Technology, 2004. **179**(2-3): p. 119-123.
70. Thaiwatthana, S., X.Y. Li, H. Dong, and T. Bell, *Comparison studies on properties of nitrogen and carbon S phase on low temperature plasma alloyed AISI 316 stainless steel.* Surface Engineering, 2002. **18**: p. 433-437.
71. A.Zielinski, J.C., B. Blaszkiewicz, *Effect of plasma nitrided layers on low-alloy steel on its hydrogen degredation.* Journal of Achievements in Materials and Manufacturing Engineering, 2006. **17**(1-2): p. 213-216.
72. McMullan, D., *Scanning electron microscopy 1928-1965.* Scanning, 1995. **17**(3): p. 175-185.
73. Michler, G.H., *Scanning Electron Microscopy (SEM)*, in *Electron Microscopy of Polymers*, P.H. Pasch, Editor. 2008, Springer-Verlag: Berlin. p. 87-88.
74. Goldstein, J. D.E.N., David C. Joy, Patrick Echlin, Charles E. Lyman, Eric Lifshin, *Scanning Electron Microscopy and X-Ray Microanalsis*. Vol. 1. 2002, Dordrecht: Kluwer Academic Publishers Group. 586.
75. Hays, C. and E.G. Kendall, *An analysis of Knoop microhardness.* Metallography, 1973. **6**(4): p. 275-282.
76. Archard, J.F. and W. Hirst, *The Wear of Metals under Unlubricated Conditions.* Proceedings of the Royal Society of London. Series A. Mathematical and Physical Sciences, 1956. **236**(1206): p. 397-410.
77. Thompson, J.M., M.K.T., *A Proposal for the Calculation of Wear*, in *2006 International ANSYS Conference Proceedings*. 2006: Pittsburgh, Pensylvania, USA. p. 14.
78. tribology-abc. *Calculation of Wear Rate*. 2010 [cited 2010 19/08/2010]; Available from: http://www.tribology-abc.com/abc/wear.htm.
79. Archard, J.F., *Contact and Rubbing of Flat Surfaces.* Journal of Applied Physics, 1953. **24**(8): p. 981-988.
80. Verbeek, H.J., *Tribological systems and wear factors.* Wear, 1979. **56**(1): p. 81-92.
81. Pistorius, P.C. and G.T. Burstein, *Metastable Pitting Corrosion of Stainless Steel and the Transition to Stability.* Philosophical Transactions: Physical Sciences and Engineering, 1992. **341**(1662): p. 531-559.
82. Kamachi Mudali, U., P. Shankar, S. Ningshen, R.K. Dayal, H.S. Khatak, and B. Raj, *On the pitting corrosion resistance of nitrogen alloyed cold worked austenitic stainless steels.* Corrosion Science, 2002. **44**(10): p. 2183-2198.
83. Czerwiec, T., N. Renevier, and H. Michel, *Low-temperature plasma-assisted nitriding.* Surface and Coatings Technology, 2000. **131**(1-3): p. 267-277.
84. Buhagiar, J., H. Dong, and T. Bell, *Low temperature plasma surface alloying of medical grade austenitic stainless steel with carbon and nitrogen.* Surface Engineering, 2007. **23**(4): p. 313-317.